Journal of General Virology (2010), 91, 122–132 DOI 10.1099/vir.0.015909-0

Requirement of cellular DDX3 for hepatitis C virus replication is unrelated to its interaction with the viral core protein

Allan G. N. Angus,[1] David Dalrymple,[1] Steeve Boulant,[1] David R. McGivern,[2] Reginald F. Clayton,[1] Martin J. Scott,[1] Richard Adair,[1] Susan Graham,[1] Ania M. Owsianka,[1] Paul Targett-Adams,[1] Kui Li,[3] Takaji Wakita,[4] John McLauchlan,[1] Stanley M. Lemon[2] and Arvind H. Patel[1]

Correspondence
Arvind H. Patel
a.patel@mrcvu.gla.ac.uk

[1]MRC Virology Unit, Institute of Virology, University of Glasgow, Church Street, Glasgow G11 5JR, UK

[2]Center for Hepatitis Research, Institute for Human Infections & Immunity, and the Department of Microbiology and Immunology, University of Texas Medical Branch, Galveston, TX 77555-0610, USA

[3]Department of Molecular Sciences, University of Tennessee Health Science Center, Memphis, TN 38163, USA

[4]Department of Virology II, National Institute of Infectious Diseases, Tokyo, Japan

The cellular DEAD-box protein DDX3 was recently shown to be essential for hepatitis C virus (HCV) replication. Prior to that, we had reported that HCV core binds to DDX3 in yeast-two hybrid and transient transfection assays. Here, we confirm by co-immunoprecipitation that this interaction occurs in cells replicating the JFH1 virus. Consistent with this result, immunofluorescence staining of infected cells revealed a dramatic redistribution of cytoplasmic DDX3 by core protein to the virus assembly sites around lipid droplets. Given this close association of DDX3 with core and lipid droplets, and its involvement in virus replication, we investigated the importance of this host factor in the virus life cycle. Mutagenesis studies located a single amino acid in the N-terminal domain of JFH1 core that when changed to alanine significantly abrogated this interaction. Surprisingly, this mutation did not alter infectious virus production and RNA replication, indicating that the core–DDX3 interaction is dispensable in the HCV life cycle. Consistent with previous studies, siRNA-led knockdown of DDX3 lowered virus production and RNA replication levels of both WT JFH1 and the mutant virus unable to bind DDX3. Thus, our study shows for the first time that the requirement of DDX3 for HCV replication is unrelated to its interaction with the viral core protein.

Received 17 August 2009
Accepted 25 September 2009

INTRODUCTION

Persistent hepatitis C virus (HCV) infection is a major cause of chronic hepatitis, cirrhosis and hepatocellular carcinoma (HCC). Current treatments for chronic infection are ineffective in approximately 50 % of patients (Chen & Morgan, 2006). The virus, which belongs to the family *Flaviviridae*, has a positive-sense RNA genome encoding a polyprotein that is cleaved by cellular and viral proteases to yield mature structural and non-structural proteins. The structural proteins are core and the envelope glycoproteins E1 and E2, while the non-structural proteins are p7, NS2, NS3, NS4A, NS4B, NS5A and NS5B (reviewed by Moradpour *et al.*, 2007). HCV exhibits a high degree of genetic variability with six distinct viral genotypes, each further divided into subtypes, and within a single individual the virus exists as a constantly evolving quasispecies (Bukh *et al.*, 1995; Pawlotsky, 2003; Simmonds, 1995).

HCV core is a highly conserved basic, RNA-binding protein that forms the viral nucleocapsid (McLauchlan, 2000). Mature core is a dimeric, alpha-helical protein that can be separated into two domains (D1 and D2) based on its hydropathic profile (Boulant *et al.*, 2005; McLauchlan, 2000). The N-terminal hydrophilic D1 domain consists of the first 117 aa and is mainly involved in RNA binding and oligomerization of the core protein (Boulant *et al.*, 2005).

Supplementary figures are available with the online version of this paper.

In addition, D1 also interacts with several cellular factors (McLauchlan, 2000). The hydrophobic D2 domain, which spans amino acid residues 118 to approximately 169, is required for correct folding of D1. D2 consists of two amphipathic α-helices connected by a hydrophobic loop and mediates core association with lipid droplets (LDs) and endoplasmic reticulum membranes (Barba *et al.*, 1997; Boulant *et al.*, 2006; Hope & McLauchlan, 2000). Recent evidence strongly suggests that the HCV core–LD association is important for the production of infectious virus particles (Boulant *et al.*, 2007; Miyanari *et al.*, 2007; Shavinskaya *et al.*, 2007).

We and others previously showed that the core domain D1 interacts with the cellular DEAD-box RNA helicase DDX3 (Mamiya & Worman, 1999; Owsianka & Patel, 1999; You *et al.*, 1999). In mammalian cells, DDX3 is present throughout the cytoplasm and can also be found in the nucleus. Ectopic expression of HCV core in these cells results in the redistribution of a proportion of DDX3 to distinct cytoplasmic sites, where it co-localizes with core. Indeed, DDX3 was recently shown to be present on LDs in core-expressing Hep39 cells (Sato *et al.*, 2006).

Cellular RNA helicases of the DEAD-box family participate in all biological processes involving RNA. They possess nine conserved motifs (see Fig. 1), including motif II (Asp–Glu–Ala–Asp or DEAD) after which the protein family is named (reviewed by Cordin *et al.*, 2006; Rocak & Linder, 2004). DDX3 is a ubiquitous cellular protein, possessing ATPase and helicase activities (Franca *et al.*, 2007; Yedavalli *et al.*, 2004). Known homologues include murine PL10 (Leroy *et al.*, 1989), *Xenopus laevis* An3 (Gururajan *et al.*, 1991) and yeast Ded1 (Jamieson & Beggs, 1991). The exact cellular function of DDX3 has yet to be defined, but there is evidence for its involvement in splicing (Deckert *et al.*, 2006; Zhou *et al.*, 2002), translation initiation and repression (Beckham *et al.*, 2008; Shih *et al.*, 2008), cell cycle regulation (Chang *et al.*, 2006; Chao *et al.*, 2006; Huang *et al.*, 2004; Sekiguchi *et al.*, 2007), nucleocytoplasmic RNA shuttling (Yedavalli *et al.*, 2004), RNA transport (Kanai *et al.*, 2004), interferon induction (Schroder *et al.*, 2008; Soulat *et al.*, 2008) and apoptosis (Sun *et al.*, 2008). Both upregulation and downregulation of DDX3 have been reported in various tumour tissues, suggesting divergent roles of DDX3 in cancer-related pathogenesis (Botlagunta *et al.*, 2008; Chang *et al.*, 2006; Chao *et al.*, 2006; Huang *et al.*, 2004).

Previously, we proposed that the HCV core–DDX3 interaction might function in virus replication and/or pathogenesis (Owsianka & Patel, 1999). Two separate studies recently provided evidence for the involvement of DDX3 in HCV replication (Ariumi *et al.*, 2007; Randall *et al.*, 2007). The importance of DDX3 in the life cycle of other viruses has also become apparent, including its requirement for human immunodeficiency virus-1 (HIV-1) replication (Yedavalli *et al.*, 2004). Furthermore, the DDX3 homologue Ded1 is required for brome mosaic virus replication (Noueiry *et al.*, 2000). In contrast, DDX3 inhibits hepatitis B virus transcription by its incorporation into nucleocapsids (Wang *et al.*, 2009). Thus, there is increasing evidence that DDX3 is important in the life cycle of several diverse viruses.

The direct relevance of the core–DDX3 interaction for the HCV life cycle has not yet been elucidated. In this study, we show that this interaction does occur in cultured cells infected with HCV strain JFH1 (Wakita *et al.*, 2005), and that DDX3 co-localizes directly with core on LDs. Using alanine substitution mutagenesis, we identified a key amino acid residue within the D1 domain of core that is

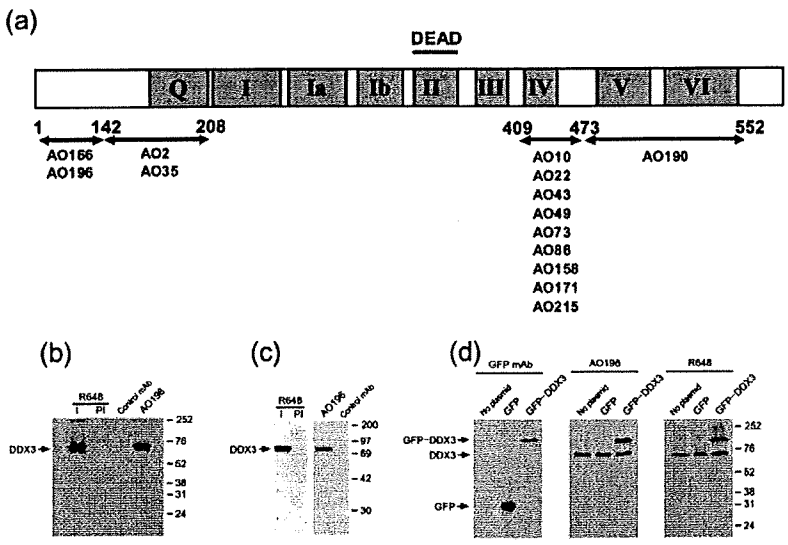

Fig. 1. Generation of anti-DDX3 antibodies. (a) Schematic representation of DDX3 protein structure showing the nine conserved motifs, including motif II (or the DEAD motif). The arrows mark the epitopes recognized by the mouse mAbs. (b) Characterization of anti-DDX3 antibodies. HuH-7 cell lysates were immunoprecipitated with the immune (I) and pre-immune (PI) antiserum R648, or mAb AO196 or an isotype control mAb. The immune complexes were analysed by Western blotting using biotinylated R648. Positions of molecular mass markers are shown (in kDa). (c) Western blotting of HuH-7 cell lysates with R648-I, -PI, mAb AO196 and isotype control mAb. (d) Western blotting of lysates of HEK cells transfected with a plasmid expressing EGFP alone or an EGFP–DDX3 fusion protein using anti-GFP mAb, AO196 and R648.

critical for this interaction. Furthermore, we examine the impact of abrogation of the core–DDX3 interaction on virus RNA replication and infectious progeny yields in cultured cells.

RESULTS

Generation of DDX3 antibodies

We previously showed that DDX3 co-localizes with HCV genotype 1a core in cytoplasmic punctate spots (Owsianka & Patel, 1999). To better understand the nature of this interaction, we generated several mouse mAbs (prefixed with 'AO', see Fig. 1a) and two rabbit polyclonal antisera (R647 and R648) to human DDX3. Both rabbit antisera and the majority of mAbs were found to interact with DDX3 by ELISA, Western blotting and immunoprecipitation assays (data not shown). The epitopes of mAbs reactive to DDX3 in Western blots were broadly mapped using truncated forms of DDX3 expressed in bacteria as GST-fusion proteins. Most of the mAbs recognized aa 409–473, a region located between motifs III and V of DDX3, whereas mAb AO190 recognized motifs V and VI. mAbs AO166 and AO196 bound to the N-terminal region, whereas mAbs AO2 and AO35 recognized the region downstream preceding the ATPase domain of DDX3 (Fig. 1a).

The specificities of antibodies AO196 and R648 for DDX3 in immunoprecipitation and Western blot assays are shown in Fig. 1(b, c, d). The polyclonal serum R648 (but not the pre-immune control serum) specifically immunoprecipitated DDX3 from a cytoplasmic extract of HuH-7 cells, as did mAb AO196 (Fig. 1b). R648 and AO196 also recognized DDX3 in cytoplasmic extracts of HuH-7 cells by Western blotting (Fig. 1c). The specificity of these antibodies was further demonstrated by their recognition of both endogenous DDX3 and an enhanced green fluorescent protein (EGFP)–DDX3 fusion protein expressed in HEK cells (Fig. 1d). mAb AO196 and R648 recognized only the cytoplasmic form of DDX3 by immunofluorescence (Fig. 2a and data not shown), even though they were able to detect DDX3 in the nuclear extracts of cells in both immunoprecipitation and Western blotting assays (data not shown). In contrast, another mAb

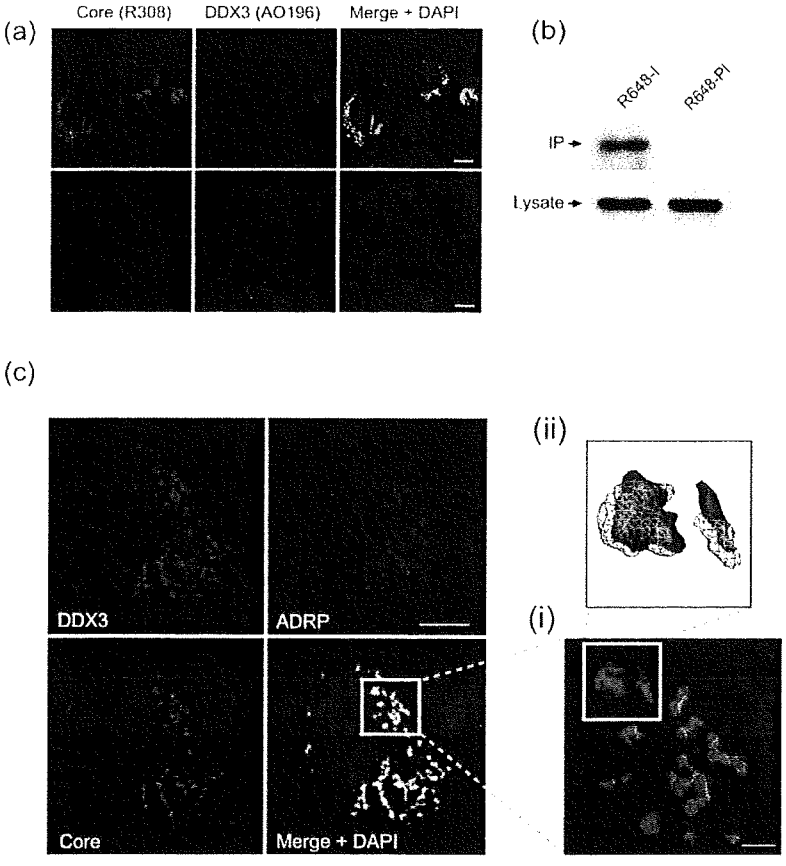

Fig. 2. Sequestration of DDX3 by HCV core. (a) DDX3 co-localizes with core in JFH1-infected cells. HuH-7 cells were either mock-infected (lower panel) or infected with JFH1 (top panel). At 3 days post-infection, cells were fixed and probed with HCV core and DDX3 using antibodies R308 and A0196, respectively. Cell nuclei were detected by counterstaining with DAPI. (b) Co-immunoprecipitation of core by anti-DDX3 antiserum. HuH-7 cells electroporated with viral RNA were lysed at 72 h post-incubation, and the lysate immunoprecipitated with anti-DDX3 R648 immune (I) or pre-immune (PI) serum. The resulting precipitates were examined by immunoblotting using anti-core mAb c7-50 (top panel). One twentieth of the cell lysate used in the co-immunoprecipitation assay was immunoblotted for core with mAb c7-50 as the input control (bottom panel). (c) Localization of DDX3 and core on LDs. HuH-7 cells electroporated with the $JFH1_{WT}$ RNA were fixed at 72 h post-transfection and probed using antibodies to core (R308), DDX3 (AO196) and ADRP. Z-stack analysis of all three proteins was performed by recording a series of approximately 20 images. 3D reconstructions of the boxed areas are shown (i) and a selected area is shown in greater detail (ii) where DDX3 is depicted as a wire frame to reveal the core–ADRP association. Bars, 10 μm for confocal images and 2 μm for 3D image.

designated AO322 recognized both the cytoplasmic and the nuclear form of DDX3 by immunofluoresence (Supplementary Fig. S1a).

HCV core interacts with cellular DDX3 in cells replicating WT JFH1

The core–DDX3 interaction was previously demonstrated in cells ectopically expressing HCV genotype 1a core, and in the absence of virus RNA replication and productive infection (Owsianka & Patel, 1999). To test whether DDX3 interacts with JFH1 core, HuH-7 cells transfected with virus RNA were first analysed by indirect immunofluorescence. DDX3 was found to be sequestered by core in JFH1-replicating cells as detected using mAbs AO196 and AO322 [Fig. 2a and Supplementary Fig. S1a (available in JGV Online), respectively]. It should be noted that the core-bound DDX3 emitted a stronger fluorescent signal compared with free DDX3 occupying the cell cytoplasm. Thus, adjustment of the core-bound DDX3 signal to prevent overexposure resulted in the apparent loss of free DDX3 from the image. A representative image of core and DDX3 in virus-infected and surrounding non-infected cells taken at two different intensities is shown in Supplementary Fig. S1(b) (available in JGV Online). The anti-DDX3 antiserum R648 specifically co-immunoprecipitated core from JFH1-replicating cells, further confirming a direct interaction between these two proteins (Fig. 2b).

We also found that DDX3 co-localized with core protein in the NNeo/C-5B(+) cell line harbouring an autonomously replicating genome-length genotype 1b RNA (Ikeda *et al.*, 2002), and HuH-7 cells infected with the intergenotypic 1a/2a chimeric virus [H-NS2/NS3 J(YH/QL)] (Yi *et al.*, 2007) (Supplementary Fig. S1c, d, available in JGV Online). Thus, the recruitment of DDX3 by core is in good agreement with our previous results (Owsianka & Patel, 1999), and is not limited to one virus genotype.

DDX3 interacts with HCV core on LDs

The association of HCV core with LDs is essential for infectious virus production (Boulant *et al.*, 2007; Miyanari *et al.*, 2007; Shavinskaya *et al.*, 2007). We sought to gain further insight into the core–DDX3 complex in the context of the JFH1 system by analysing the intracellular distribution of core and DDX3. HuH-7 cells electroporated with JFH1 RNA were analysed by indirect immunofluorescence for HCV core, DDX3 and adipocyte differentiation-related protein (ADRP), a protein abundant on the surface of LDs (Fujimoto *et al.*, 2004). As shown in Fig. 2(c) left, core associated with ADRP and the localization of DDX3 was precisely coincident with both proteins, indicating its redistribution to LDs. To examine the subcellular position of DDX3 and core in relation to ADRP in greater detail, a series of Z-stacks was obtained and used after blind deconvolution to create a three-dimensional model of LDs coated by core, ADRP and DDX3. As reported before (Boulant *et al.*, 2007), core fully coated LDs. We found that DDX3 by virtue of its interaction with core was also fully associated with LDs [Fig. 2c (i) and (ii)].

Identification of core residues required for DDX3 interaction

We previously reported that aa 1–59 of core protein are involved in its interaction with DDX3 (Owsianka & Patel, 1999). To identify critical residues within this region, a library of core 1–59 mutants containing single or multiple amino acid substitutions was generated by error-prone PCR (EP-PCR). The mutated sequences were fused in-frame with GFP and expressed in bacteria. The mutant fusion proteins were screened by incubation with GST–DDX3 fusion protein immobilized in ELISA wells, and the bound mutants detected using a rabbit polyclonal anti-GFP antiserum. Of 130 clones screened, only nine were found to be defective in binding to GST–DDX3 (data not shown). In order to confirm these results, all nine mutants were individually subcloned into a sequence encoding the HCV genotype 1a strain H77c core, E1 and E2 (pCE1E2) in a mammalian expression vector pcDNA3.1/Zeo+ (Invitrogen), and their expression was analysed by indirect immunofluorescence. The results were in accordance with the data from the initial ELISA screen in that all nine mutated core proteins failed to redistribute DDX3 (data not shown). Nucleotide sequence analysis showed that each of the mutants carried between one and four amino acid substitutions (Fig. 3). Of interest, mutant 90 had only one substitution (I30N), indicating that this residue must be required for the interaction of core with DDX3. All nine mutant proteins had at least one amino acid substitution in the region spanning residues 24–36, indicating that this region may harbour residues that are critical for the core–DDX3 interaction. To test this hypothesis, site-directed mutagenesis was carried out to revert any mutations outside of this 13 aa region back to the WT residue. These new mutant core 1–59 fragments were then subcloned into pCE1E2, and their expression analysed following transient transfection into HuH-7 cells as above. Again, none of these new core mutants redistributed DDX3 (data not shown), indicating that the 13 aa region between residues 24 and 36 of core is indeed involved in the interaction between core and DDX3. To determine which residues in this 13 aa region were essential, we carried out alanine-scanning mutagenesis across aa 24–36, individually substituting each residue in this region with alanine. As before, these alanine mutant sequences were subcloned into pCE1E2 and transiently transfected into HuH-7 cells. Immunofluorescence analysis revealed seven mutants (P25A, G26A, G28A, Q29A, V31A, G32A and L36A) that showed distinct co-localization between core and DDX3 (similar to that seen with WT HCV core), whilst the other mutants (F24A, G27A, I30A, G33A, V34A and Y35A) displayed no interaction with DDX3 at all (Supplementary Fig. S2, available in JGV Online). Thus, these results

	1 10 20 30 40 50 59
Core	MSTNPKPQPR TKRNTNRRPE DVKFPGGGQI VGGVYLLPRR GPRLGVRTTR KTSERSQPR
Mutant 25	--------K- ---------- ---------- ---G------ ---------- ------R--
Mutant 36	---------- ---------- ---------- ---D-----W ---------- -S-------
Mutant 90	---------- ---------- ---------N ---------- ---------- ---------
Mutant 99	---------- ---------- -D-------- ---D------ ---------- ---------
Mutant 110	---------- ---------- ---------N ---------- --S------- ---------
Mutant 111	-----E---- ---------- ---------- ----N----- ---------- ---------
Mutant 115	---------D -E-------- ---S------ ---------- ---------- ---------
Mutant 125	---------- -----I---- --------R- ----N----- ---------- ------R--
Mutant 126	-------H-- ---------- -----D---N -----W---- ---------- ---------

Fig. 3. Identification of core residues critical for its interaction with DDX3. Amino acid substitutions in residues 1–59 of core in nine mutants unable to interact with DDX3. Residues in the region 24–36 (shaded box) were targeted for alanine-scanning mutagenesis, which identified residues at positions 24, 27, 30, 33, 34 and 35 (underlined in the sequence at the top) that were critical for DDX3 interaction.

indicate that core residues F24, G27, I30, G33, V34 and Y35 are critical for its interaction with DDX3.

Disrupting the core–DDX3 interaction

Sequence comparison of core protein from strains H77c (genotype 1a) and JFH1 (genotype 2a) revealed 96.6% identity within the first 59 residues of core, with the key residues (F24, G27, I30, G33, V34 and Y35) for interaction with DDX3 being fully conserved (data not shown). Thus, recombinant JFH1 genomes each containing one of the six mutations were constructed. All mutants were replication competent as seen by the expression of NS5A protein at 3 days post-transfection (Fig. 4). The viral core protein in these cells was detected using two different anti-core antibodies, which bound to the mutant proteins with varying affinity. mAb c7-50 bound minimally or not at all to I30A and G33A mutants, but had increased affinity for the V34A protein. The anti-core rabbit serum R308 on the other hand recognized all core forms equally except for G33A (Fig. 4). Notably, all six core mutations are located within the epitope (aa 21–40) recognized by c7-50 (Moradpour *et al.*, 1996), which may account for the altered affinity of this mAb to some mutants. The antiserum R308 was raised against a peptide corresponding to core aa 5–25 (Hope & McLauchlan, 2000). Therefore, the smaller quantities of G33A core detected using R308 suggest either this mutation lowers the stability of the protein or simply reduces the binding efficiency of the antibody. Importantly, there was no detectable change in DDX3 protein levels in any of the transfected cell cultures tested (Fig. 4).

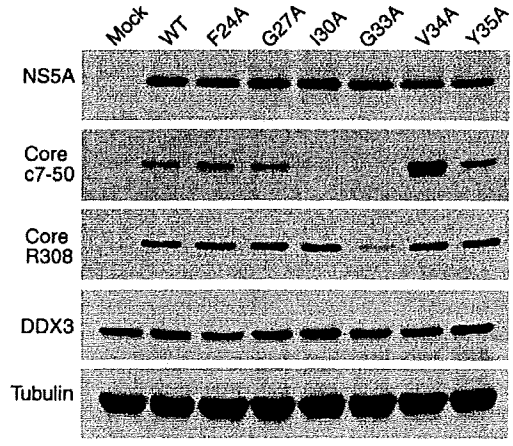

Fig. 4. Analysis of JFH1 core mutant viruses. HuH-7 cells electroporated with viral RNAs as shown were subjected to Western immunoblotting at 72 h post-incubation using anti-NS5a mAb 9E10, anti-core antibodies mAb c7-50 or R308, anti-DDX3 mAb AO196 and an anti-tubulin antibody.

We next tested by co-immunoprecipitation if these mutations had effectively disrupted the core–DDX3 interaction in virus-replicating cells. We excluded mutants I30A, G33A and V34A from this assay due to their altered affinity to mAb c7-50 (Fig. 4), which is the antibody we found to be most compatible in our co-immunoprecipitation assay. As shown in Fig. 5, the F24A and G27A core mutants were co-immunoprecipitated by the anti-DDX3 antiserum R648 in much lower amounts than the WT protein. However, the Y35A core was not co-immunoprecipated at all, indicating that its interaction with DDX3 was abrogated. Consistent with these findings, no co-localization of core and DDX3 was seen in cells replicating $JFH1_{Y35A}$ by immunofluoresence analysis (Fig. 5b). Importantly, this mutant core remained associated with LDs, which is not surprising since motifs responsible for targeting core to LDs are located in the D2 domain (Hope & McLauchlan, 2000).

HCV replication in the absence of the core–DDX3 interaction

To determine the importance of this interaction in the virus life cycle, we examined the phenotype of $JFH1_{Y35A}$.

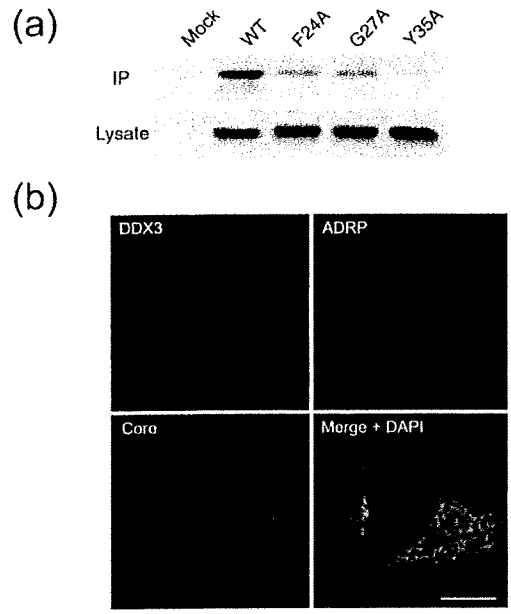

Fig. 5. Analysis of the interaction of DDX3 with core mutants. (a) HuH-7 cells were electroporated with different viral RNAs and HCV core co-immunoprecipitated at 72 h post-incubation using the anti-DDX3 serum R648 as described in the legend to Fig. 2b. (b) HuH-7 cells electroporated with $JFH1_{Y35A}$ were fixed at 72 h post-incubation and analysed by confocal microscopy for the intracellular distribution of core, DDX3 and ADRP using appropriate antibodies. Bar, 10 μm.

HuH-7 cells were electroporated with $JFH1_{WT}$, $JFH1_{Y35A}$ or the replication-deficient $JFH1_{GND}$ RNAs and incubated for various time points before determining the progeny virus yields released into the medium and intracellular viral RNA levels. As shown in Fig. 6(a), the number of infectious particles released by $JFH1_{Y35A}$-replicating cells was lower in comparison with $JFH1_{WT}$-transfected cells at 24 and 48 h post-transfection, although parity was achieved at 72 h. The intracellular RNA replication levels of $JFH1_{Y35A}$ were similar to $JFH1_{WT}$ throughout the time-course (Fig. 6b). As expected, no virus release or intracellular viral RNA replication was detected in cells harbouring $JFH1_{GND}$ RNA (Fig. 6a, b). We next examined the infectivity and replication of the core mutant virus released from electroporated cells. To do this, we infected naïve cells at an equal m.o.i. and quantified the released infectious virus progeny and the intracellular viral RNA at various times post-infection. As shown in Fig. 6(c, d), respectively, both the virus yields and RNA replication levels of $JFH1_{Y35A}$ were very similar to $JFH1_{WT}$. We found no direct reversion or second-site mutation in $JFH1_{Y35A}$ core sequence. Thus, our data indicate that the core–DDX3 interaction does not play a role in HCV morphogenesis.

Replication of HCV following siRNA-mediated knockdown of DDX3

Recent reports have shown that siRNA-mediated knockdown of DDX3 reduces $JFH1_{WT}$ replication in infected cells (Ariumi *et al.*, 2007; Randall *et al.*, 2007). To assess the influence of DDX3 abundance on virus infection in the absence of the core–DDX3 interaction, we measured the replication of $JFH1_{WT}$ and $JFH1_{Y35A}$ following infection of

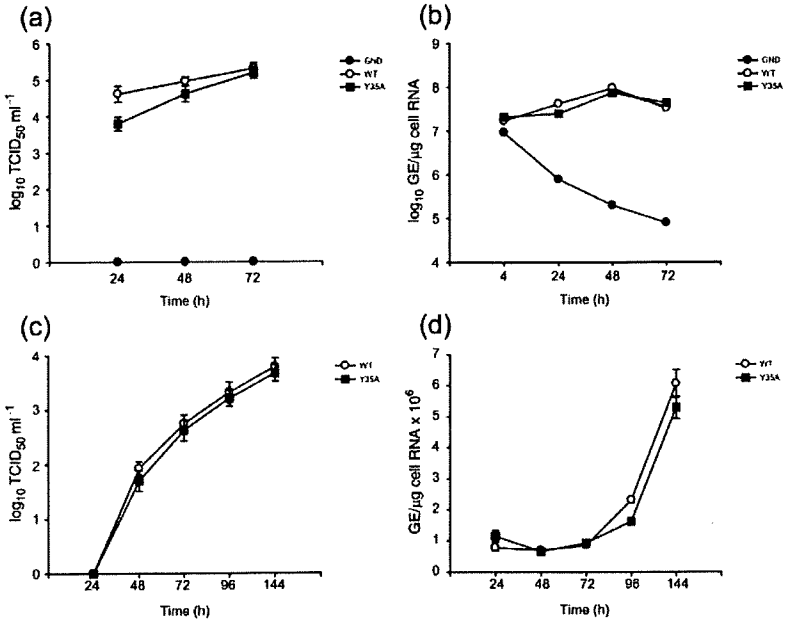

Fig. 6. Analysis of the core mutant viruses. (a, b) Determination of virus yield and intracellular RNA levels following transfection. HuH-7 cells were electroporated with RNA derived from $JFH1_{WT}$, $JFH1_{Y35A}$ or $JFH1_{GND}$ cDNA. At the indicated time points (a) the released virus titres and (b) the intracellular HCV RNA levels were quantified by $TCID_{50}$ and RT-qPCR, respectively. (c and d) Determination of virus yield and intracellular RNA levels following infection. Naïve HuH-7 cells were infected with $JFH1_{WT}$ or $JFH1_{Y35A}$ (obtained from the electroporated cells above) at an m.o.i. of 0.02. The (c) titres of infectious virus released into the medium and (d) intracellular viral RNA levels were measured over 6 days as described above. Means and error ranges from duplicate electroporations and infections are shown.

cells that had undergone efficient siRNA knockdown of DDX3 (Fig. 7a). As previously described, DDX3 knockdown cells were substantially less permissive for virus replication than normal cells following infection with $JFH1_{WT}$. Similar reductions in $JFH1_{Y35A}$ replication levels were also observed (Fig. 7b). Collectively, the data presented in Figs 6 and 7 indicate that DDX3 promotes efficient HCV infection by processes that are independent of its interaction with the viral core protein.

DISCUSSION

The recent advent of the HCV cell culture system has enabled us to further characterize the core–DDX3 interaction in the context of the complete HCV life cycle. Our overall goal is to deduce the role of DDX3 in normal cells with a view to understanding the significance of its interaction with HCV core in the virus life cycle and pathogenesis. Towards this end, we generated a large panel of mAbs recognizing different regions of DDX3. Using a subset of these, we confirmed that this interaction is genuine in JFH1-infected cells.

Given the putative function of DDX3 in RNA metabolism, initial identification of the core–DDX3 interaction led us and others to postulate its possible role in virus replication and assembly (Mamiya & Worman, 1999; Owsianka & Patel, 1999; You *et al.*, 1999). Recent data using the JFH1 system suggest that HCV RNA replication and virus assembly occur in LD-associated membranes (Boulant *et al.*, 2007; Miyanari *et al.*, 2007). Core protein, which associates with LDs (McLauchlan, 2000; Roingeard & Hourioux, 2008), recruits the viral non-structural proteins, replication complexes and envelope glycoproteins to these sites, allowing virus assembly to proceed in this local environment (Miyanari *et al.*, 2007). We show here that core also recruits the cellular DDX3 to LDs, suggesting that it may have a function in HCV replication. In keeping with this, two recent studies have shown reductions in JFH1 replication when DDX3 is removed from the cell by siRNA (Ariumi *et al.*, 2007; Randall *et al.*, 2007). We hypothesized that disrupting the association between HCV core and DDX3 might be detrimental to HCV replication, and provide insights into the purpose of this interaction. Our mutagenesis analysis revealed that the Y35A substitution in the JFH1 core molecule abrogated this interaction without affecting core–LD association. No alteration to virus RNA replication, translation or infectious particle production was observed following transfection of this mutant viral RNA into the cells. Similarly, $JFH1_{Y35A}$ virus yields from cells infected with the mutant progeny were equivalent to those of the WT virus. Interestingly, the two other mutants identified in this study ($JFH1_{F24A}$ and $JFH1_{G27A}$) showed greater reductions in virus replication, particularly post-infection (Supplementary Fig. S3, available in JGV Online). However, given their interaction with DDX3 is only slightly reduced (Fig. 5), this impairment is unlikely to be related to the disruption of the core–DDX3 interaction. A more plausible explanation for their unusual phenotypes could be an alteration in core function and/or RNA structure resulting from an alanine substitution at these positions, and as such these mutants require further investigations. Nevertheless, our results collectively suggest that the core–DDX3 interaction plays no role in virus morphogenesis.

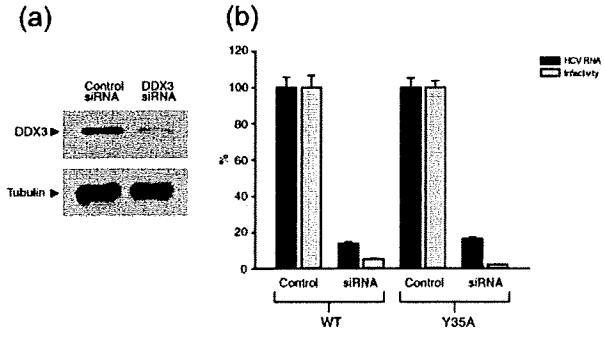

Fig. 7. Infection of DDX3 knockdown cells. (a) HuH-7 cells were transfected with siRNA duplexes as indicated. Cells were harvested after 2 days and examined by Western blotting using the anti-DDX3 mAb AO196. (b) Naïve and DDX3-deficient HuH-7 cells were infected with WT $JFH1_{WT}$ or $JFH1_{Y35A}$ virus. At 2 days post-infection the levels of released virus and intracellular HCV RNA were measured by $TCID_{50}$ assay and RT-qPCR, respectively. Means and error ranges from duplicate infections are shown.

Subgenomic replicons that do not possess core replicate as well as, if not better than, replicons encoding the entire polyprotein (Blight *et al.*, 2000; Ikeda *et al.*, 2002; Lohmann *et al.*, 1999), which indicates that the core–DDX3 interaction per se is not essential for HCV RNA replication. Nevertheless, Ariumi *et al.* (2007) reported that subgenomic replicons showed a twofold decrease in RNA replication in DDX3 knockdown cells. This finding raises an intriguing prospect that DDX3 may play a direct role in HCV RNA replication independent of and in addition to its interaction with core. Nonetheless, these workers observed a much greater reduction in JFH1 RNA replication in cells supporting replication of full genome-length RNAs, indicating greater importance of DDX3 in this setting and supporting the functional relevance of the interaction of DDX3 with core. We reproduced the deleterious effects of DDX3 knockdown on the $JFH1_{WT}$ replication but also found a similar phenotype for $JFH1_{Y35A}$ (Fig. 7). This finding further supports the notion of the core–DDX3 interaction having no function in HCV replication. Therefore, our data make a clear distinction between the effects of siRNA knockdown of DDX3 from the cells and disruption of the core–DDX3 interaction on HCV replication.

The possible involvement of the core–DDX3 interaction in pathogenesis cannot be discounted. Indeed, core protein has been widely implicated in modulating cellular functions, mainly due to its interaction with numerous host

factors (McLauchlan, 2000; Ray & Ray, 2001; Watashi & Shimotohno, 2003). Differential regulation of DDX3 has been reported in a number of tumours, including HCC, suggesting that it may be involved in HCV-associated pathogenesis (Botlagunta *et al.*, 2008; Chang *et al.*, 2006; Chao *et al.*, 2006; Huang *et al.*, 2004). DDX3 is also one of several DEAD-box proteins that are upregulated during HIV-1 replication (Krishnan & Zeichner, 2004). Interestingly, it is also upregulated during immune response to lipopolysaccharide-induced inflammation and during interferon treatment (de Veer *et al.*, 2001; Saban *et al.*, 2006). Thus, it is possible that during active viral replication HCV recruits DDX3 protein to evade host immune recognition, thereby adversely affecting one or more of its roles in normal cells (Rosner & Rinkevich, 2007) and in turn contributing to viral pathogenesis. Although we observed no differences in DDX3 expression levels between JFH1-infected cultured cells and uninfected cells, its relevance *in vivo* from a long-term disease perspective warrants further investigation.

METHODS

Cell culture and antibodies. Human hepatoma HuH-7 (Nakabayashi *et al.*, 1982) cells were propagated as described previously (Witteveldt *et al.*, 2009). The anti-NS5A mouse monoclonal antibody (mAb) 9E10 was a kind gift from Charles M. Rice (Center for the Study of Hepatitis C, The Rockefeller University, New York, USA) (Lindenbach *et al.*, 2005). The anti-HCV core rabbit serum R308, and the anti-ADRP sheep serum have been described previously (Hope & McLauchlan, 2000; Targett-Adams *et al.*, 2003). The anti-HCV core mAb c7-50 and the anti-α-tubulin and anti-GFP mAbs were purchased from Bioreagents and Sigma, respectively.

Generation and characterization of anti-DDX3 antibodies. BALB/c mice and rabbits were immunized with a bacterially expressed glutathione *S*-transferase-full-length DDX3 (GST–DDX3) fusion protein and antibodies generated essentially as previously described (Clayton *et al.*, 2002). A total of two rabbit polyclonal antisera (R647 and R648) and 16 mouse hybridomas secreting mAbs (see Fig. 1) to DDX3 was generated. The mAbs were initially identified and selected on the basis of their ability to interact with GST–DDX3, but not an irrelevant GST fusion protein, in an ELISA assay (data not shown).

Plasmid constructs and mutagenesis. The full-length DDX3 gene was cloned into the *Bam*HI site, in-frame to sequences encoding the EGFP, in the vector pEGFP-C1 (Clontech) to generate EGFP–DDX3 fusion protein.

To identify residues within the N-terminal 59 aa of HCV core that are critical for interaction with DDX3, EP-PCR was performed to introduce random mutations into the HCV genotype 1a strain H77c (Yanagi *et al.*, 1997) sequence encoding this region. The fidelity of *Taq* polymerase was decreased by altering the relative dNTP concentrations, using a high Mg^{2+} concentration and including Mn^{2+} in the reaction as described previously (Pritchard *et al.*, 2005). The mutated sequences were cloned in-frame with (and downstream of) green fluorescence protein (GFP) in the bacterial expression vector pKK223-3 (Pharmacia) and the library of core 1–59 mutant–GFP fusion proteins generated was screened in an *in vitro* DDX3-binding assay as described in Results. Nucleotide sequencing subsequently identified the mutations introduced by EP-PCR in the clones of interest.

The plasmid pUC-JFH1 carries the full-length cDNA of the genotype 2a HCV strain JFH1 (Wakita *et al.*, 2005). The plasmids pUC-GND JFH1 and pUC-JFH1 ΔE1E2 are identical except that they carry the GND mutation in the NS5B-encoding sequence, or an in-frame deletion in the E1 and E2 sequences (Wakita *et al.*, 2005). Site-directed mutagenesis was carried out using the QuikChange-II kit (Stratagene) to introduce alanine substitutions at the target sites in core. Briefly, various alanine substitutions in the core-coding region were individually introduced into the plasmid pGEM-T (Promega) carrying nt 1–2614 (corresponding to the 5′ UTR and core to E2 coding sequence) of HCV strain JFH1 using appropriate primers (the sequences of which are available upon request). The presence of the desired mutation in the resulting clones was confirmed by nucleotide sequencing. Sequences carrying the appropriate mutation were subcloned back into pJFH1-pUC to generate mutant viruses (see below).

Generation of JFH1 virus and its mutated derivatives. Ten micrograms of RNA synthesized *in vitro* using linearized plasmid templates carrying the wild-type (WT) or mutated JFH1 genomic cDNA was electroporated into HuH-7 cells as described previously (Wakita *et al.*, 2005). The electroporated cells were seeded into appropriate tissue culture dishes and incubated at 37 °C. At the indicated time period, the medium containing the infectious virus progeny was filtered through a 0.45 μm pore-sized membrane and infectivity determined as described below.

Determination of virus infectivity and RNA replication. Virus titres in the culture supernatants were determined as $TCID_{50}$ (Lindenbach *et al.*, 2005) following immunostaining for NS5A. The intracellular and extracellular HCV RNA content was measured by reverse transcription-quantitative real-time-polymerase chain reaction (RT-qPCR) as described previously (Witteveldt *et al.*, 2009). To determine virus replication after electroporation, cells transfected with the respective transcript were seeded into 10 cm culture dishes, incubated at 37 °C for 4 h and then trypsinized. Total RNA was prepared from 1/15 of the trypsinized cells using the RNeasy kit (Qiagen) to quantify viral RNA by qRT-PCR assay. The remaining cell suspension was split 1 : 3 into three T25 flasks. Following incubation at 37 °C for 24, 48 and 72 h, the infectious virus yields in cell culture supernatants were determined by $TCID_{50}$ assay and the intracellular viral RNA levels quantified by RT-qPCR. To measure virus replication after infection, 5.3×10^3 naïve HuH-7 cells seeded into six-well culture dishes were infected with virus at the indicated m.o.i. Following incubation at 37 °C for 24, 48, 72, 96 and 144 h, infectious virus yields and intracellular viral RNA levels were determined as described above.

SDS-PAGE and Western blotting. Cell lysates were subjected to SDS-PAGE followed by Western blotting using appropriate antibodies as described previously (Clayton *et al.*, 2002). The bound antibodies were detected using enhanced chemiluminescence reagents (Amersham).

Immunoprecipitation of DDX3. HuH-7 cells were washed with PBS, lysed in lysis buffer (20 mM Tris/HCl pH 7.4, 20 mM iodoacetamide, 150 mM NaCl, 1 mM EDTA and 0.5 % Triton X-100) and the lysate was spun briefly to remove nuclei. The clarified cell lysates were incubated with the anti-DDX3 antibodies as described in the text and the immune complexes precipitated using protein G agarose beads (Sigma). Following washes of the Sepharose beads, the immune complexes were analysed by SDS-PAGE followed by Western blotting using biotinylated R648 and anti-streptavidin-horseradish peroxidase (HRP) conjugate.

Co-immunoprecipitation of HCV core protein. Approximately, 5×10^6 HuH-7 cells electroporated with viral RNA were seeded into

100 mm tissue culture dishes. At 72 h post-transfection, the cells were washed and lysed in 0.5 ml lysis buffer (20 mM Tris/HCl, pH 7.4, 135 mM NaCl and 0.1 % Triton X-100) supplemented with 50 mM NAF, 5 mM Na_3VO_4 and 1 mM PMSF. The lysate was spun briefly to remove nuclei. After pre-clearing, the clarified lysate was immunoprecipitated overnight with protein G agarose beads that had been pre-incubated with the anti-DDX3 antiserum R648. The beads carrying the immune complex were spun at 2000 r.p.m. (microcentrifuge) for 2 min, washed three times with the lysis buffer and subjected to non-reducing SDS-PAGE followed by Western blotting using the anti-core mAb c7-50 and anti-mouse IgG-HRP conjugate.

Indirect immunofluorescence. Cells on coverslips were fixed in methanol and probed with the indicated primary antibody for 1 h at room temperature. After washing with PBS, cells were incubated with anti-species antibodies conjugated with fluorescein isothiocyanate, tetramethyl rhodamine isothiocyanate or Cy5 (Invitrogen) for 1 h and then washed with PBS. The coverslips were examined with a Zeiss Laser Scanning LSM510 META inverted confocal microscope (Carl Zeiss) and the images analysed using LSM510 software. Three-dimensional (3D) reconstructions were performed from Z-stack images collected using optimum intervals. Image stacks were deconvolved by 3D-blind deconvolution using Autodeblur software (MediaCybernetics), and 3D reconstructions were generated as described previously (Boulant *et al.*, 2007; Targett-Adams *et al.*, 2008).

RNA interference. Two pre-validated siRNA duplexes (s4004 and s4005, synthesized by Applied Biosystems) targeting different regions of the human DDX3 and a negative control siRNA composed of a scrambled sequence were used. Naïve HuH-7 cells plated overnight were transfected with lipofectamine RNAiMax (Invitrogen) and 50 nM siRNAs according to the manufacturer's protocol. The cells were then incubated for a further 2 days prior to virus infection. The efficiency of DDX3 knockdown was determined by immunoblotting using mAb AO196.

ACKNOWLEDGEMENTS

We thank Duncan McGeoch for helpful criticism of this manuscript and Charles M. Rice for the anti-NS5A mAb 9E10. This work was funded in part by grants from the Medical Research Council, UK (A. H. P.), Marie Curie Intra-European Fellowship contract 025198 (S. B.), the National Institute of Allergy and Infectious Diseases, U19-AI40035 (S. M. L.) and by the National Institute of Health, AI069285 (K. L.).

REFERENCES

Ariumi, Y., Kuroki, M., Abe, K., Dansako, H., Ikeda, M., Wakita, T. & Kato, N. (2007). DDX3 DEAD-box RNA helicase is required for hepatitis C virus RNA replication. *J Virol* **81**, 13922–13926.

Barba, G., Harper, F., Harada, T., Kohara, M., Goulinet, S., Matsuura, Y., Eder, G., Schaff, Z., Chapman, M. J. & other authors (1997). Hepatitis C virus core protein shows a cytoplasmic localization and associates to cellular lipid storage droplets. *Proc Natl Acad Sci U S A* **94**, 1200–1205.

Beckham, C., Hilliker, A., Cziko, A. M., Noueiry, A., Ramaswami, M. & Parker, R. (2008). The DEAD-Box RNA helicase Ded1p affects and accumulates in *Saccharomyces cerevisiae* P-bodies. *Mol Biol Cell* **19**, 984–993.

Blight, K. J., Kolykhalov, A. A. & Rice, C. M. (2000). Efficient initiation of HCV RNA replication in cell culture. *Science* **290**, 1972–1974.

Botlagunta, M., Vesuna, F., Mironchik, Y., Raman, A., Lisok, A., Winnard, P., Jr, Mukadam, S., Van Diest, P., Chen, J. H. & other authors (2008). Oncogenic role of DDX3 in breast cancer biogenesis. *Oncogene* **27**, 3912–3922.

Boulant, S., Vanbelle, C., Ebel, C., Penin, F. & Lavergne, J. P. (2005). Hepatitis C virus core protein is a dimeric alpha-helical protein exhibiting membrane protein features. *J Virol* **79**, 11353–11365.

Boulant, S., Montserret, R., Hope, R. G., Ratinier, M., Targett-Adams, P., Lavergne, J. P., Penin, F. & McLauchlan, J. (2006). Structural determinants that target the hepatitis C virus core protein to lipid droplets. *J Biol Chem* **281**, 22236–22247.

Boulant, S., Targett-Adams, P. & McLauchlan, J. (2007). Disrupting the association of hepatitis C virus core protein with lipid droplets correlates with a loss in production of infectious virus. *J Gen Virol* **88**, 2204–2213.

Bukh, J., Miller, R. H. & Purcell, R. H. (1995). Genetic heterogeneity of hepatitis C virus: quasispecies and genotypes. *Semin Liver Dis* **15**, 41–63.

Chang, P. C., Chi, C. W., Chau, G. Y., Li, F. Y., Tsai, Y. H., Wu, J. C. & Wu Lee, Y. H. (2006). DDX3, a DEAD box RNA helicase, is deregulated in hepatitis virus-associated hepatocellular carcinoma and is involved in cell growth control. *Oncogene* **25**, 1991–2003.

Chao, C. H., Chen, C. M., Cheng, P. L., Shih, J. W., Tsou, A. P. & Lee, Y. H. (2006). DDX3, a DEAD box RNA helicase with tumor growth-suppressive property and transcriptional regulation activity of the p21waf1/cip1 promoter, is a candidate tumor suppressor. *Cancer Res* **66**, 6579–6588.

Chen, S. L. & Morgan, T. R. (2006). The natural history of hepatitis C virus (HCV) infection. *Int J Med Sci* **3**, 47–52.

Clayton, R. F., Owsianka, A., Aitken, J., Graham, S., Bhella, D. & Patel, A. H. (2002). Analysis of antigenicity and topology of E2 glycoprotein present on recombinant hepatitis C virus-like particles. *J Virol* **76**, 7672–7682.

Cordin, O., Banroques, J., Tanner, N. K. & Linder, P. (2006). The DEAD-box protein family of RNA helicases. *Gene* **367**, 17–37.

Deckert, J., Hartmuth, K., Boehringer, D., Behzadnia, N., Will, C. L., Kastner, B., Stark, H., Urlaub, H. & Luhrmann, R. (2006). Protein composition and electron microscopy structure of affinity-purified human spliceosomal B complexes isolated under physiological conditions. *Mol Cell Biol* **26**, 5528–5543.

de Veer, M. J., Holko, M., Frevel, M., Walker, E., Der, S., Paranjape, J. M., Silverman, R. H. & Williams, B. R. (2001). Functional classification of interferon-stimulated genes identified using microarrays. *J Leukoc Biol* **69**, 912–920.

Franca, R., Belfiore, A., Spadari, S. & Maga, G. (2007). Human DEAD-box ATPase DDX3 shows a relaxed nucleoside substrate specificity. *Proteins* **67**, 1128–1137.

Fujimoto, Y., Itabe, H., Sakai, J., Makita, M., Noda, J., Mori, M., Higashi, Y., Kojima, S. & Takano, T. (2004). Identification of major proteins in the lipid droplet-enriched fraction isolated from the human hepatocyte cell line HuH7. *Biochim Biophys Acta* **1644**, 47–59.

Gururajan, R., Perry-O'Keefe, H., Melton, D. A. & Weeks, D. L. (1991). The *Xenopus* localized messenger RNA An3 may encode an ATP-dependent RNA helicase. *Nature* **349**, 717–719.

Hope, R. G. & McLauchlan, J. (2000). Sequence motifs required for lipid droplet association and protein stability are unique to the hepatitis C virus core protein. *J Gen Virol* **81**, 1913–1925.

Huang, J. S., Chao, C. C., Su, T. L., Yeh, S. H., Chen, D. S., Chen, C. T., Chen, P. J. & Jou, Y. S. (2004). Diverse cellular transformation capability of overexpressed genes in human hepatocellular carcinoma. *Biochem Biophys Res Commun* **315**, 950–958.

Ikeda, M., Yi, M., Li, K. & Lemon, S. M. (2002). Selectable subgenomic and genome-length dicistronic RNAs derived from an infectious molecular clone of the HCV-N strain of hepatitis C virus replicate efficiently in cultured Huh7 cells. *J Virol* **76**, 2997–3006.

Jamieson, D. J. & Beggs, J. D. (1991). A suppressor of yeast spp81/ded1 mutations encodes a very similar putative ATP-dependent RNA helicase. *Mol Microbiol* **5**, 805–812.

Kanai, Y., Dohmae, N. & Hirokawa, N. (2004). Kinesin transports RNA: isolation and characterization of an RNA-transporting granule. *Neuron* **43**, 513–525.

Krishnan, V. & Zeichner, S. L. (2004). Alterations in the expression of DEAD-box and other RNA binding proteins during HIV-1 replication. *Retrovirology* **1**, 42.

Leroy, P., Alzari, P., Sassoon, D., Wolgemuth, D. & Fellous, M. (1989). The protein encoded by a murine male germ cell-specific transcript is a putative ATP-dependent RNA helicase. *Cell* **57**, 549–559.

Lindenbach, B. D., Evans, M. J., Syder, A. J., Wolk, B., Tellinghuisen, T. L., Liu, C. C., Maruyama, T., Hynes, R. O., Burton, D. R. & other authors (2005). Complete replication of hepatitis C virus in cell culture. *Science* **309**, 623–626.

Lohmann, V., Korner, F., Koch, J., Herian, U., Theilmann, L. & Bartenschlager, R. (1999). Replication of subgenomic hepatitis C virus RNAs in a hepatoma cell line. *Science* **285**, 110–113.

Mamiya, N. & Worman, H. J. (1999). Hepatitis C virus core protein binds to a DEAD box RNA helicase. *J Biol Chem* **274**, 15751–15756.

McLauchlan, J. (2000). Properties of the hepatitis C virus core protein: a structural protein that modulates cellular processes. *J Viral Hepat* **7**, 2–14.

Miyanari, Y., Atsuzawa, K., Usuda, N., Watashi, K., Hishiki, T., Zayas, M., Bartenschlager, R., Wakita, T., Hijikata, M. & Shimotohno, K. (2007). The lipid droplet is an important organelle for hepatitis C virus production. *Nat Cell Biol* **9**, 1089–1097.

Moradpour, D., Wakita, T., Tokushige, K., Carlson, R. I., Krawczynski, K. & Wands, J. R. (1996). Characterization of three novel monoclonal antibodies against hepatitis C virus core protein. *J Med Virol* **48**, 234–241.

Moradpour, D., Penin, F. & Rice, C. M. (2007). Replication of hepatitis C virus. *Nat Rev Microbiol* **5**, 453–463.

Nakabayashi, H., Taketa, K., Miyano, K., Yamane, T. & Sato, J. (1982). Growth of human hepatoma cells lines with differentiated functions in chemically defined medium. *Cancer Res* **42**, 3858–3863.

Noueiry, A. O., Chen, J. & Ahlquist, P. (2000). A mutant allele of essential, general translation initiation factor DED1 selectively inhibits translation of a viral mRNA. *Proc Natl Acad Sci U S A* **97**, 12985–12990.

Owsianka, A. M. & Patel, A. H. (1999). Hepatitis C virus core protein interacts with a human DEAD box protein DDX3. *Virology* **257**, 330–340.

Pawlotsky, J. M. (2003). Hepatitis C virus genetic variability: pathogenic and clinical implications. *Clin Liver Dis* **7**, 45–66.

Pritchard, L., Corne, D., Kell, D., Rowland, J. & Winson, M. (2005). A general model of error-prone PCR. *J Theor Biol* **234**, 497–509.

Randall, G., Panis, M., Cooper, J. D., Tellinghuisen, T. L., Sukhodolets, K. E., Pfeffer, S., Landthaler, M., Landgraf, P., Kan, S. & other authors (2007). Cellular cofactors affecting hepatitis C virus infection and replication. *Proc Natl Acad Sci U S A* **104**, 12884–12889.

Ray, R. B. & Ray, R. (2001). Hepatitis C virus core protein: intriguing properties and functional relevance. *FEMS Microbiol Lett* **202**, 149–156.

Rocak, S. & Linder, P. (2004). DEAD-box proteins: the driving forces behind RNA metabolism. *Nat Rev Mol Cell Biol* **5**, 232–241.

Roingeard, P. & Hourioux, C. (2008). Hepatitis C virus core protein, lipid droplets and steatosis. *J Viral Hepat* **15**, 157–164.

Rosner, A. & Rinkevich, B. (2007). The DDX3 subfamily of the DEAD box helicases: divergent roles as unveiled by studying different organisms and in vitro assays. *Curr Med Chem* **14**, 2517–2525.

Saban, M. R., Hellmich, H. L., Turner, M., Nguyen, N. B., Vadigepalli, R., Dyer, D. W., Hurst, R. E., Centola, M. & Saban, R. (2006). The inflammatory and normal transcriptome of mouse bladder detrusor and mucosa. *BMC Physiol* **6**, 1.

Sato, S., Fukasawa, M., Yamakawa, Y., Natsume, T., Suzuki, T., Shoji, I., Aizaki, H., Miyamura, T. & Nishijima, M. (2006). Proteomic profiling of lipid droplet proteins in hepatoma cell lines expressing hepatitis C virus core protein. *J Biochem* **139**, 921–930.

Schroder, M., Baran, M. & Bowie, A. G. (2008). Viral targeting of DEAD box protein 3 reveals its role in TBK1/IKKε-mediated IRF activation. *EMBO J* **27**, 2147–2157.

Sekiguchi, T., Kurihara, Y. & Fukumura, J. (2007). Phosphorylation of threonine 204 of DEAD-box RNA helicase DDX3 by cyclin B/cdc2 in vitro. *Biochem Biophys Res Commun* **356**, 668–673.

Shavinskaya, A., Boulant, S., Penin, F., McLauchlan, J. & Bartenschlager, R. (2007). The lipid droplet binding domain of hepatitis C virus core protein is a major determinant for efficient virus assembly. *J Biol Chem* **282**, 37158–37169.

Shih, J. W., Tsai, T. Y., Chao, C. H. & Wu Lee, Y. H. (2008). Candidate tumor suppressor DDX3 RNA helicase specifically represses cap-dependent translation by acting as an eIF4E inhibitory protein. *Oncogene* **27**, 700–714.

Simmonds, P. (1995). Variability of hepatitis C virus. *Hepatology* **21**, 570–583.

Soulat, D., Burckstummer, T., Westermayer, S., Goncalves, A., Bauch, A., Stefanovic, A., Hantschel, O., Bennett, K. L., Decker, T. & Superti-Furga, G. (2008). The DEAD-box helicase DDX3X is a critical component of the TANK-binding kinase 1-dependent innate immune response. *EMBO J* **27**, 2135–2146.

Sun, M., Song, L., Li, Y., Zhou, T. & Jope, R. S. (2008). Identification of an antiapoptotic protein complex at death receptors. *Cell Death Differ* **15**, 1887–1900.

Targett-Adams, P., Chambers, D., Gledhill, S., Hope, R. G., Coy, J. F., Girod, A. & McLauchlan, J. (2003). Live cell analysis and targeting of the lipid droplet-binding adipocyte differentiation-related protein. *J Biol Chem* **278**, 15998–16007.

Targett-Adams, P., Boulant, S. & McLauchlan, J. (2008). Visualization of double-stranded RNA in cells supporting hepatitis C virus RNA replication. *J Virol* **82**, 2182–2195.

Wakita, T., Pietschmann, T., Kato, T., Date, T., Miyamoto, M., Zhao, Z., Murthy, K., Habermann, A., Krausslich, H. G. & other authors (2005). Production of infectious hepatitis C virus in tissue culture from a cloned viral genome. *Nat Med* **11**, 791–796.

Wang, H., Kim, S. & Ryu, W. S. (2009). DDX3 DEAD-Box RNA helicase inhibits hepatitis B virus reverse transcription by incorporation into nucleocapsids. *J Virol* **83**, 5815–5824.

Watashi, K. & Shimotohno, K. (2003). The roles of hepatitis C virus proteins in modulation of cellular functions: a novel action mechanism of the HCV core protein on gene regulation by nuclear hormone receptors. *Cancer Sci* **94**, 937–943.

Witteveldt, J., Evans, M. J., Bitzegeio, J., Koutsoudakis, G., Owsianka, A. M., Angus, A. G., Keck, Z. Y., Foung, S. K., Pietschmann, T. & other authors (2009). CD81 is dispensable for

hepatitis C virus cell-to-cell transmission in hepatoma cells. *J Gen Virol* **90**, 48–58.

Yanagi, M., Purcell, R. H., Emerson, S. U. & Bukh, J. (1997). Transcripts from a single full-length cDNA clone of hepatitis C virus are infectious when directly transfected into the liver of a chimpanzee. *Proc Natl Acad Sci U S A* **94**, 8738–8743.

Yedavalli, V. S., Neuveut, C., Chi, Y. H., Kleiman, L. & Jeang, K. T. (2004). Requirement of DDX3 DEAD box RNA helicase for HIV-1 Rev-RRE export function. *Cell* **119**, 381–392.

Yi, M., Ma, Y., Yates, J. & Lemon, S. M. (2007). Compensatory mutations in E1, p7, NS2, and NS3 enhance yields of cell culture-infectious intergenotypic chimeric hepatitis C virus. *J Virol* **81**, 629–638.

You, L. R., Chen, C. M., Yeh, T. S., Tsai, T. Y., Mai, R. T., Lin, C. H. & Lee, Y. H. (1999). Hepatitis C virus core protein interacts with cellular putative RNA helicase. *J Virol* **73**, 2841–2853.

Zhou, Z., Licklider, L. J., Gygi, S. P. & Reed, R. (2002). Comprehensive proteomic analysis of the human spliceosome. *Nature* **419**, 182–185.

THE JOURNAL OF BIOLOGICAL CHEMISTRY VOL. 285, NO. 2, pp. 845–854, January 8, 2010

Ethanol Enhances Hepatitis C Virus Replication through Lipid Metabolism and Elevated NADH/NAD$^+$*

Received for publication, July 17, 2009, and in revised form, October 30, 2009 Published, JBC Papers in Press, November 12, 2009, DOI 10.1074/jbc.M109.045740

Scott Seronello[‡], Chieri Ito[‡], Takaji Wakita[§], and Jinah Choi[‡1]

From the [‡]School of Natural Sciences, University of California, Merced, Atwater, California 95343 and the [§]National Institute of Infectious Diseases, Tokyo 162-8640, Japan

Ethanol has been suggested to elevate HCV titer in patients and to increase HCV RNA in replicon cells, suggesting that HCV replication is increased in the presence and absence of the complete viral replication cycle, but the mechanisms remain unclear. In this study, we use Huh7 human hepatoma cells that naturally express comparable levels of CYP2E1 as human liver to demonstrate that ethanol, at subtoxic and physiologically relevant concentrations, enhances complete HCV replication. The viral RNA genome replication is affected for both genotypes 2a and 1b. Acetaldehyde, a major product of ethanol metabolism, likewise enhances HCV replication at physiological concentrations. The potentiation of HCV replication by ethanol is suppressed by inhibiting CYP2E1 or aldehyde dehydrogenase and requires an elevated NADH/NAD$^+$ ratio. In addition, acetate, isopropyl alcohol, and concentrations of acetone that occur in diabetics enhance HCV replication with corresponding increases in the NADH/NAD$^+$. Furthermore, inhibiting the host mevalonate pathway with lovastatin or fluvastatin and fatty acid synthesis with 5-(tetradecyloxy)-2-furoic acid or cerulenin significantly attenuates the enhancement of HCV replication by ethanol, acetaldehyde, acetone, as well as acetate, whereas inhibiting β-oxidation with β-mercaptopropionic acid increases HCV replication. Ethanol, acetaldehyde, acetone, and acetate increase the total intracellular cholesterol content, which is attenuated with lovastatin. In contrast, both endogenous and exogenous ROS suppress the replication of HCV genotype 2a, as previously shown with genotype 1b. Conclusion: Therefore, lipid metabolism and alteration of cellular NADH/NAD$^+$ ratio are likely to play a critical role in the potentiation of HCV replication by ethanol rather than oxidative stress.

Ethanol consumption is a well-known risk factor for chronic liver diseases. Ethanol is also a key cofactor in the pathogenesis induced by hepatitis C virus (HCV),[2] and it decreases the efficacy of anti-HCV treatments (1, 2). Likewise, HCV infection exacerbates liver damage caused by prolonged alcohol abuse (2). It has also been reported that patients with a history of alcohol abuse are more likely to be infected with HCV than the rest of the population (1).

In addition, ethanol has been suggested to exacerbate HCV-induced liver diseases in part by affecting the viral titer (2–5). Hepatitis C patients who drink alcohol typically show a pattern of hepatic injury that is more characteristic of chronic viral hepatitis than alcohol-induced injury, suggesting that alcohol enhances the pathogenic effects of HCV rather than exerting its independent effects on liver (6). Several clinical studies have correlated increased serum and intrahepatic HCV titer with the amount of alcohol consumed (2, 4, 5). Abstinence or moderation of alcohol consumption could reduce the HCV titer in some patients (2, 5). Furthermore, *in vitro* studies suggest that ethanol increases HCV RNA levels in Huh7 human hepatoma replicon cell lines that continuously support the HCV RNA replication without virus production (3, 7, 8). These studies suggest that ethanol enhances HCV replication both in the presence and absence of the complete viral replication cycle. HCV replicon systems and more recent virus-producing cell culture models have increased our understanding of HCV and provide us with tools for studying potential interactions between HCV and pathological cofactors, such as ethanol (9).

Nevertheless, whether ethanol directly enhances HCV production in the context of the complete viral replication cycle has not been demonstrated. Furthermore, the mechanism by which ethanol modulates HCV RNA replication remains controversial as reactive oxygen species (ROS) and lipid peroxidation products, which can be generated during ethanol metabolism, can suppress, rather than increase, HCV RNA replication in cells, suggesting the involvement of other metabolites of ethanol (10–14). Oxidative hepatic ethanol metabolism is a multistep process (4). Alcohol dehydrogenase, the predominant ethanol-metabolizing enzyme, is found in the cytosol and produces acetaldehyde and NADH. Ethanol-inducible cytochrome P450 (CYP2E1), which is induced during extended ethanol exposure, is another major ethanol-metabolizing enzyme located in the endoplasmic reticulum and generates NADP$^+$ and ROS in addition to acetaldehyde. Catalase, which is found in peroxisomes, is thought to not contribute significantly to ethanol metabolism under normal conditions. Once ethanol is metabolized into acetaldehyde, it is rapidly converted into acetate and NADH by aldehyde dehydrogenase. Acetaldehyde and other products of ethanol metabolism have been implicated in many pathogenic effects of ethanol. Whether these metabolites also

* This work was supported by start-up funds from the University of California, Merced (to J. C.).

[1] To whom correspondence should be addressed: School of Natural Sciences, University of California, Merced, 5200 N. Lake Rd, Merced, CA 95343. Tel.: 209-228-4386; Fax: 209-228-4060; E-mail: jchoi@ucmerced.edu.

[2] The abbreviations used are: HCV, hepatitis C virus; ROS, reactive oxygen species; nt, nucleotides; GAPDH, glyceraldehyde-3-phosphate dehydrogenase; qRT-PCR, quantitative reverse transcriptase-polymerase chain reaction; siRNA, small interfering RNA; IRES, internal ribosomal entry site; DADS, diallyl disulfide; BSO, L-buthionine *S,R*-sulfoximine; GSH, glutathione; GO, glucose oxidase; NAC, *N*-acetylcysteine; 4MP, 4-methylpyrazole; TOFA, 5-(tetradecyloxy)-2-furoic acid.

participate in the modulation of HCV replication by ethanol, however, has not yet been tested.

Therefore, the goal of this study was to determine the effects of ethanol exposure on HCV replication in the context of the complete HCV replication cycle and the mechanisms, comparing the effects of other metabolites of ethanol with those of ROS. Our data show that ethanol and acetaldehyde, at subtoxic and physiologically relevant concentrations, elevate complete HCV replication, as opposed to the suppression caused by endogenous and exogenous ROS. Our data further suggest that elevation of the ratio of NADH/NAD^+ and modulation of lipid metabolism are likely to play critical roles in the modulation of HCV replication by ethanol. Possible implications on *in vivo* HCV replication, patient education, and disease management are also discussed.

EXPERIMENTAL PROCEDURES

HCV Constructs—The genotype 2a HCV constructs, pJFH1 (produces infectious virus particles), replicative-null pJFH1-GND, and subgenomic pSgJFH1-Luc (contains a luciferase reporter gene), are described elsewhere (15, 16). Huh7 cell clones (SgPC2 and Clone B) supporting continuous replication of a subgenomic HCV replicon of genotype 1b (Con1 sequence) were also used (11, 17). The subgenomic replicons support HCV RNA replication but no virus is formed.

HCV RNA Transfection, Infection, and Cell Culture—The *in vitro* transcription, transfection of HCV RNA, and Huh7 human hepatoma cell culture were performed as described (10, 11). For the *in vitro* infectivity assays, 2 ml of the extracellular medium from JFH1 RNA-transfected cells were used to inoculate naïve Huh7 or Huh7.5 cells with 3 ml of fresh medium, as described (16, 18). Treatments were initiated 24 h after infection, and the cells were harvested after another 24 or 48 h.

Northern Blot Analysis—Intracellular RNA extraction and Northern blots were carried out, as described (10, 11). DNA probes were prepared from nucleotides (nt) 4128–8273 or 358–2816 of JFH1, generated with ScaI and ApaL I, respectively, or 3669 to 6016 of the Con1 subgenomic replicons. Images were quantified by densitometry, using Optiquant Cyclone 4.00 (Perkin Elmer), and data were normalized by glyceraldehyde-3-phosphate dehydrogenase (GAPDH) mRNA content.

Quantitative Real-time Reverse Transcriptase-Polymerase Chain Reaction (qRT-PCR)—The total intracellular RNA was obtained from cells using TRIzol (Invitrogen). To obtain extracellular HCV RNA, cell culture medium samples were first treated with RNase A (100 μg/ml) for 30 min at room temperature, then RNA was extracted using TRIzol LS, and glycogen as a carrier. HCV RNA was quantified by qRT-PCR as described (11, 16). The primer sequences for JFH1 were 5′-TCTGCGGAACCGGTGAGTA-3′ (nt 146–164; forward), and 5′-TCAGGCAGTACCACAAGGC-3′ (nt 277–295; reverse), and the sequence of the fluorogenic probe, labeled with 6-FAM and TAMRA (Biosearch Technologies, Inc.), was 5′-CCAGTCTTCCCGGCAATTCCG-3′ (nt 168–188). Standard curves were generated using *in vitro* transcribed HCV RNA. Intracellular HCV RNA levels were normalized by 18 S rRNA or GAPDH mRNA.

Western Blot Analysis—Cells were sonicated in Laemmli buffer, and proteins were analyzed for NS5A and β-actin by Western blot, as described (10). Loading was normalized by protein assay of acetone-precipitated proteins determined with the bicinchoninic acid assay kit (Pierce). Quantification of Western blots was performed by densitometry using the Kodak IS2000R software.

Luciferase Assays—After various treatments, SgJFH1Luc RNA-transfected cells were lysed with 1× Reporter Lysis Buffer, and the luciferase activity was determined using Luciferase Reporter Assay kit (Promega) (15). Luciferase activities were normalized by total protein content, determined with bicinchoninic acid assay kit (Pierce).

In Vitro HCV Replication Assay—In vitro replication assay was carried out, as previously described (10, 11). Briefly, cytoplasmic lysates were prepared, and the replication was allowed to proceed for 1 h at 30 °C in the presence of [α-^{32}P]CTP and actinomycin D. Then, RNA products were analyzed on a 1% formaldehyde-agarose gel, which was subsequently analyzed, using Optiquant Cyclone 4.00 (PerkinElmer Life Sciences).

CYP2E1 Small Interfering RNA (siRNA)—Huh7 and SgPC2 cells were transfected with 50 nM CYP2E1 (Santa Cruz Biotechnology) or non-targeting control (Dharmacon) siRNAs, using RNAiMax (Invitrogen) per the manufacturer's recommendations.

CYP2E1 Activity Assay—Cells were treated with and without 0.2% ethanol for 48 h and lysed. CYP2E1 activity was determined by measuring hydroxylation of *p*-nitrophenol as described, except NADPH, instead of the NADPH-generating system, was used (19). The specificity was demonstrated by inhibiting the reaction with 100 μM CYP2E1 antibodies, and portion of the activity that is inhibited by CYP2E1 antibodies was then calculated and reported.

NADH/NAD^+, Cholesterol, and ATP Assays—NADH and NAD^+ levels were determined by enzymatic NADH recycling assay, using the NAD^+/NADH Quantification kit from Biovision, per the manufacturer's recommendations. After various treatments, cells were collected in 400 μl of NADH/NAD^+ extraction buffer. Samples were immediately subjected to two freeze/thaw cycles and filtered using Microcon YM-10 (Millipore). Then, the samples were split into two sets, one of which was used to carry out the thermal decomposition of NAD^+ followed by the cycling assay for the determination of NADH content of the cell. The other set was used to measure the total NADH plus NAD^+ content by performing the cycling assay without the thermal decomposition. Then, the NADH/NAD^+ ratio was calculated. Total intracellular cholesterol was measured using the Cholesterol/Cholesteryl Ester Quantitation kit (Biovision) per the manufacturer's instructions. Briefly, cells were homogenized in chloroform/isopropyl alcohol/Triton X-100 (7:11:0.1). The lipids were extracted, and all traces of organic solvents were evaporated prior to resuspending the lipids in the reaction buffer and performing the assay. Total ATP content was measured using Somatic Cell ATP Assay kit (Sigma-Aldrich). The data were normalized by total protein content, determined with the bicinchoninic acid assay kit (Pierce).

Statistics—Data were analyzed using Student's *t* test or one-way analysis of variance, using SigmaStat 3.1 (Jandel Scientific).

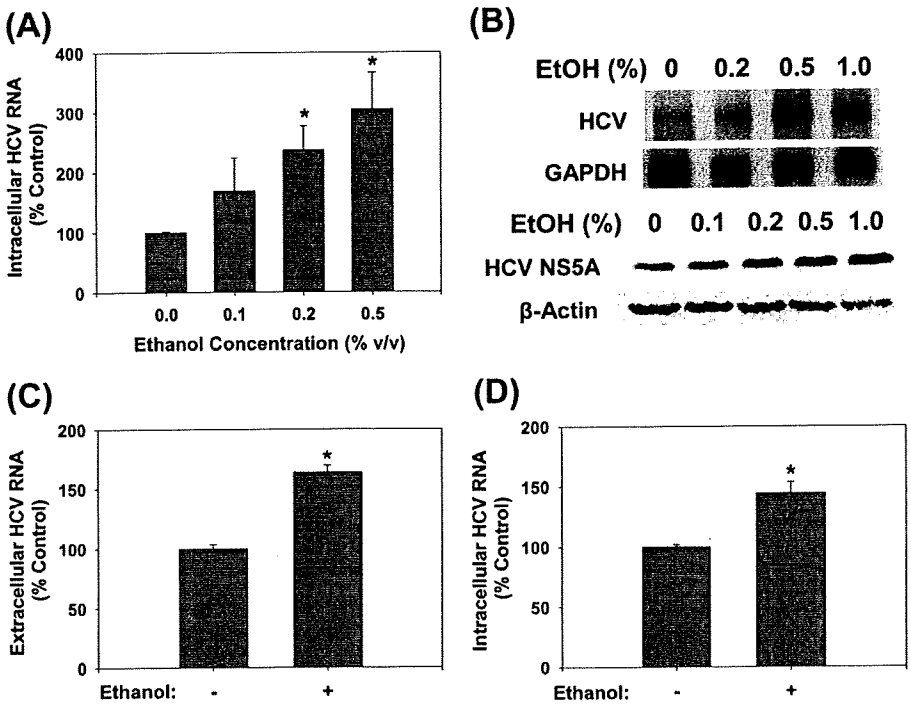

FIGURE 1. **Ethanol increases JFH1 replication.** Huh7 cells transfected with JFH1 RNA were analyzed for intracellular HCV RNA by (*A*) qRT-PCR ($n = 6$) or (*B*) Northern blots ($n = 4$) and for HCV NS5A protein content by Western blot ($n = 3$) (*B, bottom panel*) after 48 h of ethanol treatments. *C*, extracellular HCV RNA levels were analyzed by qRT-PCR for 0.2% ethanol treatments ($n = 4$). *D*, naïve Huh7 cells were inoculated with virus-containing medium and analyzed for HCV RNA after 48 h of 0.2% ethanol treatment ($n = 4$). *, indicates statistically significant difference for indicated sample sizes ($p < 0.05$).

A p value ≤ 0.05 was considered significant. All experiments were repeated three to six times, and either the means ± S.E. of several independent experiments or the representative Northern or Western blot images are shown.

RESULTS

Ethanol Increases the Complete Replication of HCV at Physiological Concentrations—To examine whether ethanol increased the complete replication of HCV, positive-sense genomic JFH1 RNA was produced by *in vitro* transcription using T7 RNA polymerase and transfected into Huh7 human hepatoma cells. Then, the transfected cells were exposed to 0–1.0% (v/v, 0–172 mM) ethanol once daily for 48 h. Then, the cells and the cell culture medium were harvested and analyzed for intracellular and RNase A-resistant extracellular HCV RNAs by a combination of Northern blots and qRT-PCR. Ethanol significantly increased the intracellular JFH1 HCV RNA levels to 237 ± 40 and 305 ± 61% of untreated controls at 0.2 and 0.5% concentrations, respectively ($p < 0.05$) (Fig. 1, *A* and *B, top panel*). HCV NS5A protein level similarly increased with ethanol treatments (Fig. 1*B, bottom panel*). Extracellular HCV RNA was also significantly elevated with the 0.2% ethanol treatment, indicating increased virus secretion (Fig. 1*C*). Next, we examined whether virus-infected cells responded similarly to ethanol treatment with elevated HCV RNA. We found that 0.2% ethanol also increased HCV RNA in Huh7 cells infected with cell culture-generated JFH1 virions (Fig. 1*D*). JFH1 GND mutant, which harbors a critical mutation (GDD:GND) in NS5B, the viral polymerase, did not replicate or generate infectious virus particles, as expected (data not shown). These concentrations of ethanol did not induce any cytotoxicity, as assessed by cell morphology and measuring the ATP content (data not shown). The 0.2% ethanol, equivalent to blood alcohol concentration of 34.4 mM, that significantly enhanced HCV replication, is approximately twice the legal limit for driving under the influence in many countries, including the United States. The 0.5% ethanol lies in the toxic range but can also be achieved physiologically, particularly in chronic alcohol users. In addition, ethanol is volatile, and the amount that remains would be significantly less than what was added to cell culture medium (20). These data, therefore, suggest that ethanol can enhance complete HCV replication, at physiologically attainable concentrations.

Ethanol Enhances HCV RNA Replication of Genotypes 2a and 1b—Previously, ethanol was shown to elevate HCV RNA content in Huh7 cells that supported subgenomic HCV RNA replication without virus production (3, 7, 8). To test whether the JFH1 RNA replication was also affected by ethanol, we transfected Huh7 cells with SgJFH1-Luc RNA and exposed the cells to ethanol for 48 h. Then, HCV replication was monitored by measuring the firefly luciferase activity (15). Ethanol increased the luciferase activity in these cells, suggesting that the JFH1 RNA genome replication was affected (Fig. 2*A*).

Genotype 2a HCV infection is found globally, with the prevalence ranging from less than 2 to about 30% depending on the geographical region (21, 22). However, as the most prevalent HCV genotype is genotype 1, we also repeated these experiments, using Con1 subgenomic replicon (SgPC2) cells (11, 17). Again, significant increases in the genotype 1b HCV RNA could be demonstrated with 0.1–1% ethanol (Fig. 2*B, top panel*). Similar increases in the HCV NS5A protein content was demonstrated by Western blots (Fig. 2*B, bottom panel*).

To confirm that the rate of the HCV RNA genome replication is accelerated by ethanol, we measured the activity of the HCV RNA replication complex. JFH1-transfected cells were exposed to ethanol for 5 h and then, the cytoplasmic lysates, containing the HCV replication complex, were isolated. Then, the *in vitro* RNA replication assay was performed in the presence of α-^{32}P-labeled CTP and actinomycin D, as previously described (11). JFH1 cell extracts produced a single band that corresponded to the expected size of the HCV RNA, indicating active viral RNA replication, whereas the JFH1 GND extracts did not (Fig. 2*C*). Ethanol significantly increased the rate of

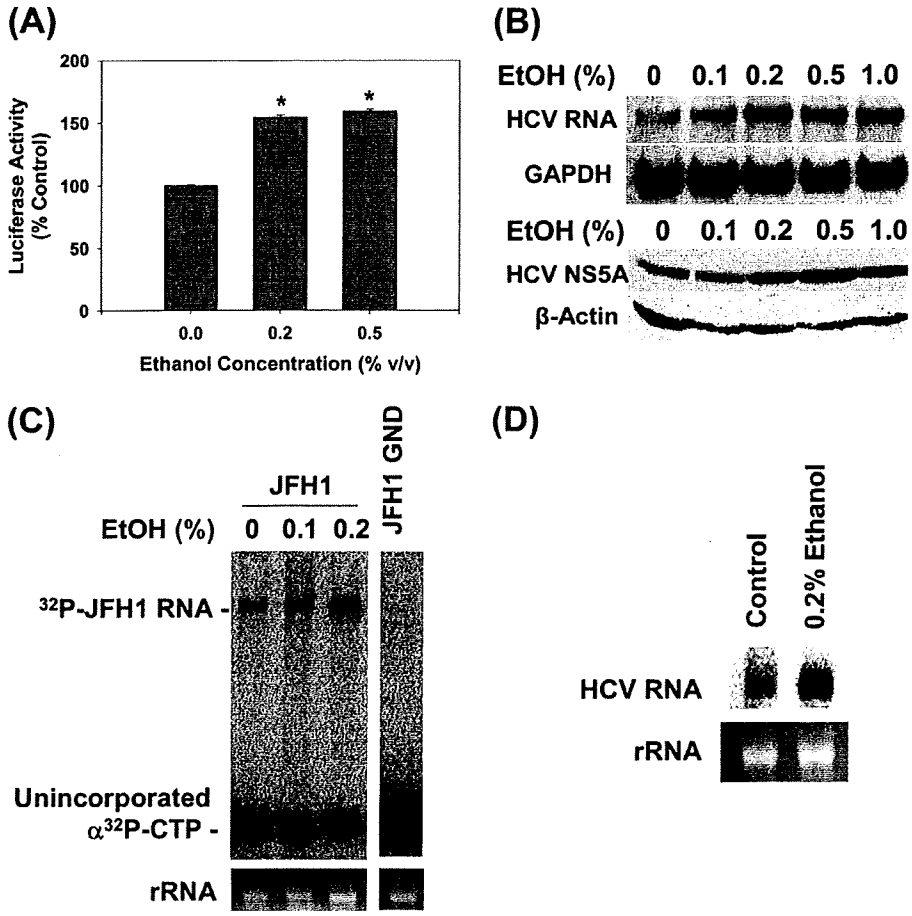

FIGURE 2. **Ethanol increases the replication of subgenomic JFH1 and Con1 replicon RNAs.** *A*, Huh7 cells transfected with SgJFH1-Luc RNA were analyzed for luciferase activity after 48-h ethanol treatments ($n = 3$). *B*, stable Huh7 clones expressing SgCon1-Neo (SgPC2) were incubated with ethanol for 24 h and analyzed for HCV RNA, GAPDH mRNA, and NS5A and β-actin proteins ($n = 3$) by Northern and Western blots, respectively ($n = 3$). *C* and *D*, cytosolic lysates were prepared from (*C*) JFH1 and JFH1-GND RNA-transfected cells and (*D*) SgPC2 cells, after 5 h of ethanol treatment, these lysates were used to carry out *in vitro* replication assays ($n = 3$). *Bottom panels* show ethidium bromide staining of rRNA as the loading control. *, indicates statistically significant difference for indicated sample sizes ($p < 0.05$).

HCV RNA replication (Fig. 2*C*). Ethanol also accelerated the *in vitro* replication rate of Con1 strain (Fig. 2*D*). On the other hand, ethanol did not increase the HCV internal ribosomal entry site (IRES) activity, as assessed by the HCV IRES activity assay, using pRL-HL (data not shown) (23). The data suggest that ethanol increases the rate of HCV RNA replication without directly enhancing its translation rate, at least when these processes are evaluated separately. Therefore, increases in the NS5A protein content with ethanol (Fig. 2*B*) are likely to have resulted from increased levels of the viral RNA template available for translation.

CYP2E1 Is Present in Huh7 Cells at Significant Levels as in Human Liver—Next, we started examining the mechanism by which ethanol increased HCV replication, first, by identifying key steps of ethanol metabolism that mediated this effect (Fig. 3*A*). Alcohol dehydrogenase I was not detected in significant levels in our Huh7 cells (data not shown). To confirm that ethanol metabolism is occurring in our cells, we then analyzed our Huh7 cells for the expression of CYP2E1. Our Huh7 cells expressed significant levels of CYP2E1 protein, which was about 2.2 ± 0.5-fold less than human liver (Fig. 3*B*). CYP2E1 expression could also be enhanced by 1.5 ± 0.2-fold with daily treatment with 0.2% (v/v) ethanol for 48 h (Fig. 3*C*). This enhanced expression of CYP2E1 could be maintained for at least 2 weeks. The CYP2E1 activities (Fig. 3*D*) were within the expected range for human liver, which is 0.25–3.3 nmol/min/mg protein, and paralleled the CYP2E1 expression levels (Fig. 3*C*) (19). CYP2E1 activity of human liver shown in Fig. 3*B* was 1.83 ± 0.01 nmol/min/mg. Con1 SgPC2 cells had similar expression and activity levels of CYP2E1 as Huh7 cells (0.81 ± 0.02 nmol/min/mg without ethanol; 1.01 ± 0.06 nmol/min/mg with 0.2% ethanol).

The ethanol-induced potentiation of HCV replication could be abrogated with 25 μM diallyl disulfide (DADS), an inhibitor of CYP2E1 (Fig. 3*E*). In addition, CYP2E1 siRNA, which decreased CYP2E1 protein level to 35 ± 9% ($p < 0.05$) of the controls transfected with non-targeting control siRNA, also significantly blunted the potentiation of HCV replication by ethanol (Fig. 3*E*). These data suggest that ethanol is being metabolized by these cells, and that CYP2E1 activity is critical for the potentiation of HCV replication by ethanol in our system.

ROS Suppresses JFH1 Replication—Hepatic ethanol, particularly CYP2E1-mediated, metabolism generates ROS in addition to acetaldehyde (24) (Fig. 3*A*) and previously, we showed that ROS could suppress subgenomic Con1 and H77c/Con1 hybrid HCV RNA replication in these cells (10, 11). To resolve these seemingly conflicting observations, we continued to examine how ROS affected JFH1. To examine the effects of endogenously generated ROS, we first used L-buthionine *S,R*-sulfoximine (BSO). BSO depletes glutathione (GSH), a major endogenous antioxidant, by inhibiting its *de novo* synthesis. Therefore, BSO would amplify the effects of endogenous ROS, generated during normal cellular metabolism and in response to HCV (4). BSO decreased intracellular GSH content by ~80 ± 12% in Huh7 cells ($p < 0.05$). In addition, BSO decreased both intracellular and extracellular JFH1 RNA levels (Fig. 4, *A* and *B*). To confirm that BSO was acting specifically by decreasing GSH, cells were treated with BSO and GSH ethyl ester, which enters cells and is cleaved by cellular esterases to restore GSH inside cells, bypassing the inhibition of GSH biosynthesis by BSO. GSH ethyl ester partially restored both intracellular and extracellular HCV RNA (Fig. 4, *A* and *B*).

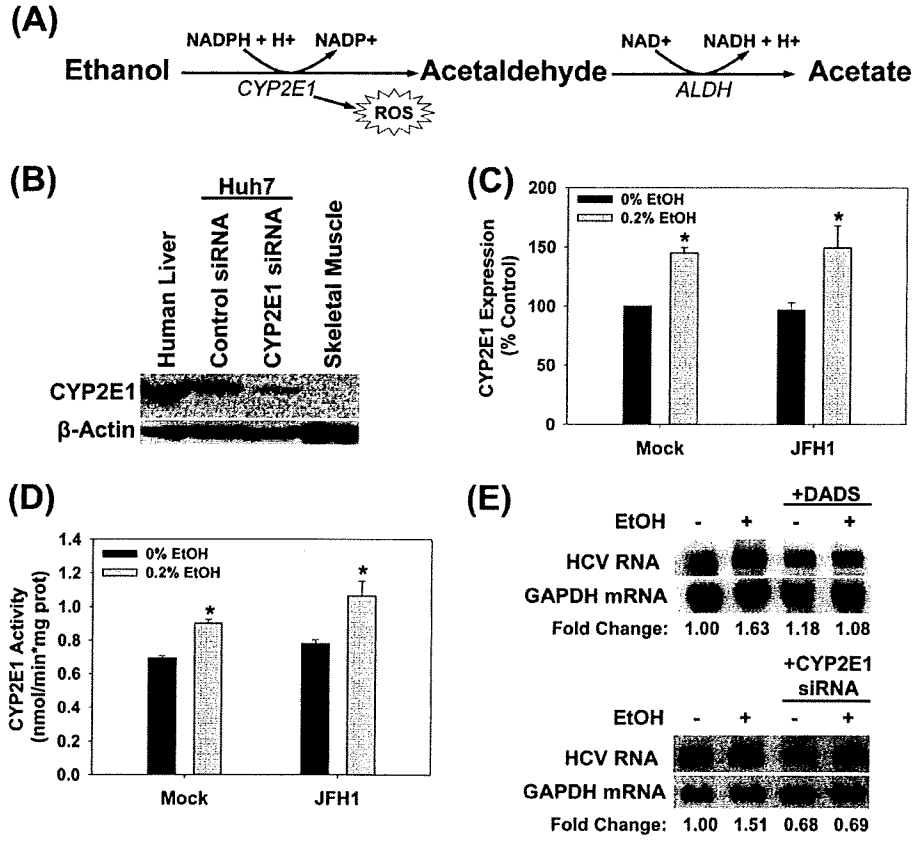

FIGURE 3. **CYP2E1 expression in Huh7 cells.** *A*, CYP2E1-dependent ethanol metabolism. *B*, human liver tissue, Huh7 cells transfected with 50 μM non-targeting control or CYP2E1 siRNA, and skeletal muscle tissue were analyzed for CYP2E1 protein content by Western blot ($n = 3$). *C* and *D*, mock- or JFH1-transfected Huh7 cells were incubated with or without 0.2% (v/v) ethanol for 48 h and analyzed for (*C*) CYP2E1 expression by Western blot ($n = 3$) and (*D*) CYP2E1-dependent *p*-nitrophenol hydroxylation activity ($n = 3$). *E*, SgPC2 cells were exposed to 0.2% ethanol ± 25 μM DADS for 24 h or transfected with 50 nM control or CYP2E1 siRNA for 24 h and then incubated with ethanol for 24 h and analyzed for HCV RNA by Northern blot ($n = 3$). *, indicates statistically significant difference for indicated sample sizes ($p < 0.05$).

Adding extracellular GSH, which is broken down into its constituents, then taken up for intracellular *de novo* GSH synthesis, and does not bypass the BSO-inhibited step, could not restore the HCV RNA level in these cells, as expected. The data suggest that BSO decreases HCV replication specifically by decreasing GSH.

To examine the effects of the exogenous ROS, JFH1 RNA-transfected cells were incubated with 0.25 milliunits/ml of glucose oxidase (GO), which produces H_2O_2 extracellularly through an enzymatic reaction in the presence of glucose, mimicking ROS generation during inflammation. GO decreased the intracellular JFH1 RNA by 30 ± 8% ($p < 0.05$) and exacerbated the suppression of HCV RNA by BSO (Fig. 4*C*). In addition, JFH1 RNA levels decreased with 25, 50, and 100 μM H_2O_2 (Fig. 4*D*). Treating cells with BSO plus GO or either agent alone likewise suppressed the subgenomic JFH1 RNA replication (Fig. 4*E*). BSO and H_2O_2 also countered the enhancement of HCV replication by ethanol (Fig. 4*F*). Furthermore, *N*-acetylcysteine (NAC) and Trolox, a water soluble vitamin E, either increased or had no significant effect on the ethanol-induced enhancement of HCV replication (Fig. 4*G*). These cell treatments did not induce cytotoxicity, as determined by the ATP assay (data not shown). Thus, ROS were not likely to be responsible for the potentiation of HCV RNA replication by ethanol. These data are consistent with the suppression of HCV RNA replication previously observed with HCV genotype 1 (10, 11).

Acetaldehyde Increases the Replication of HCV—We next evaluated whether another major product of ethanol metabolism, acetaldehyde, had similar effects on HCV as ethanol. Acetaldehyde, at physiologically relevant concentrations (25), significantly increased the HCV RNA content in both non-virus producing and virus-producing JFH1 cells (Fig. 5, *A* and *B*). Infecting naïve cells with virus-containing medium and then treating with 5 μM acetaldehyde also led to significant increases in HCV replication (Fig. 5*C*). To examine whether acetaldehyde had similar effects on genotype 1b HCV, SgPC2 cells were also incubated with acetaldehyde and analyzed for changes in HCV replication. Acetaldehyde likewise elevated the HCV RNA level in these cells (Fig. 5*D*). Another Con1 HCV subgenomic replicon cell clone, Clone B, derived in another laboratory (17), responded similarly to ethanol and acetaldehyde, indicating that the response is not specific to our cell clone (Fig. 5*D*). Thus, acetaldehyde is sufficient to potentiate HCV replication of both genotypes 1b and 2a.

Isopropyl Alcohol and Acetone Also Potentiate HCV Replication, the Role of NADH/NAD$^+$—We continued to investigate whether acetaldehyde itself or products of acetaldehyde metabolism are critical for the potentiation of HCV replication by ethanol by inhibiting aldehyde dehydrogenase with cyanamide (see Fig. 3*A*). Cyanamide suppressed the potentiation of HCV replication by ethanol just as inhibiting the first step of ethanol metabolism with 4-methylpyrazole (4MP) and DADS did, suggesting that it is not acetaldehyde itself but a downstream product of acetaldehyde metabolism that increases HCV replication (Fig. 6*A*, *left panel*).

Acetaldehyde metabolism by aldehyde dehydrogenase generates NADH and acetate (Fig. 3*A*). To determine the potential role of NADH, we first evaluated the effects of isopropyl alcohol. Isopropyl alcohol (0.2%, v/v) increases the levels of NADH like ethanol but generates acetone instead of acetaldehyde. To our surprise, isopropyl alcohol also increased the HCV RNA level (Fig. 6*B*, *left panel*) (26). Both isopropyl alcohol and ethanol increased NADH/NAD$^+$ ratio in these cells, as expected

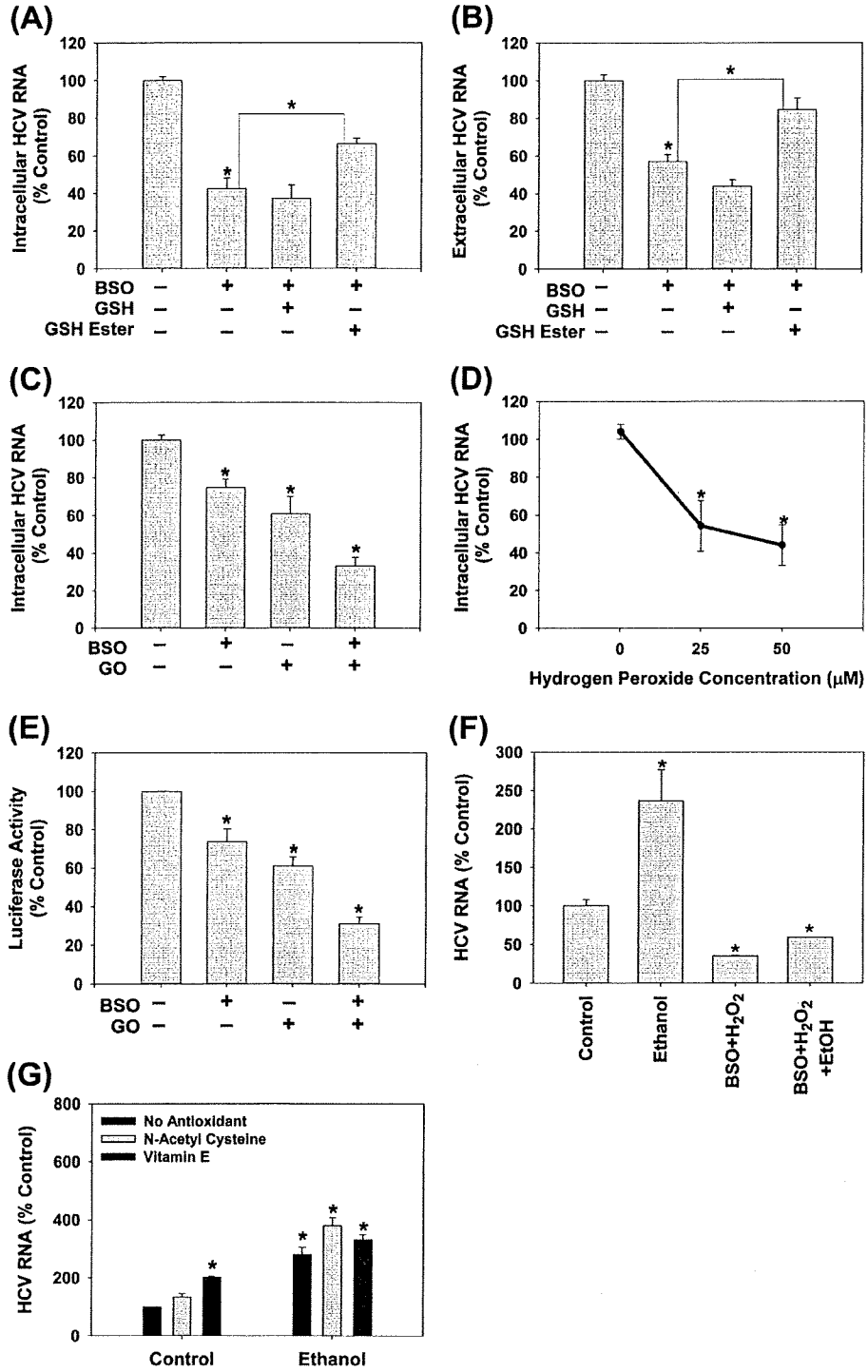

FIGURE 4. **Endogenous and exogenous ROS suppress HCV replication.** JFH1-transfected Huh7 cells were treated with BSO with and without 2 mM GSH or GSH ester (*A* and *B*) ($n = 3$), GO + glucose with and without 16 h of pretreatment with 20 μM BSO (*C*) ($n = 4$), or bolus H_2O_2 (*D*) ($n = 4$) for 24 h. Then, JFH1 intracellular (*A*, *C*, *D*) and extracellular (*B*) HCV RNA levels were analyzed by qRT-PCR. *E*, Huh7 cells transfected with SgJFH1-Luc RNA were assayed for luciferase activity after 24 h treatment with 0.25 milliunits/ml glucose oxidase + glucose with and without the BSO pretreatment ($n = 3$). *F*, SgPC2 cells were treated with 0.2% ethanol ± H_2O_2 plus BSO for 24 h, and analyzed for HCV RNA and GAPDH mRNA by Northern blot. *G*, SgPC2 cells were treated for 24 h with ethanol ± 5 mM NAC or 0.5 μM Trolox (water-soluble vitamin E). Then, HCV RNA and GAPDH mRNA levels were monitored by Northern blot and quantified by densitometry ($n = 3$). *, indicates statistically significant difference for indicated sample sizes ($p < 0.05$).

(Fig. 6*B*, *right panel*). In contrast, *tert*-butanol did not elevate HCV replication or the NADH/NAD^+ ratio (Fig. 6*B*).

Moreover, we found that acetate itself increased the level of HCV RNA as treating cells with acetone also did. In addition, ethanol, acetaldehyde, acetate, isopropyl alcohol, and acetone all showed corresponding increases in NADH/NAD^+ ratios (Fig. 6*B*, *right panel*) (4, 27). The NADH/NAD^+ ratios were positively correlated with HCV RNA content in all of these treatments ($r = 0.95$, $p < 0.001$) (Fig. 6*B*). The suppression of HCV replication by cyanamide, 4MP, and DADS in Fig. 6*A* (*left panel*) was also associated with corresponding decreases in the NADH/NAD^+ ratios (Fig. 6*A*, *right panel*). Therefore, changes in HCV replication paralleled the changes in the NADH/NAD^+ ratio, produced by these treatments.

Then, we examined whether increased NADH/NAD^+ ratio was required for the potentiation of HCV replication by ethanol and these other agents. Pyruvate, which re-oxidizes cytosolic NADH to NAD^+, completely abrogated the increases in HCV replication and NADH levels during ethanol, acetaldehyde, acetate, isopropyl alcohol, and acetone treatments (Fig. 6*C*). Methylene blue, which also oxidizes NADH, had similar effects on HCV as pyruvate (data not shown). In contrast, lactate, which produces NADH in the cytosol independent of ethanol, increased NADH levels to 235.9 ± 11.9% ($p < 0.05$) of the control level but had little to no effect on HCV replication (Fig. 6*D*). Together, these data indicate that whereas an alteration of cellular NADH/NAD^+ levels seems necessary for the ethanol-induced increases in HCV replication, elevated NADH/NAD^+ may not be sufficient to increase HCV replication.

The Potentiation of HCV Replication by Ethanol Requires Lipogenesis—NADH has diverse functions in the cell, and one of these functions includes modulation of lipid metabolism. For example, NADH can

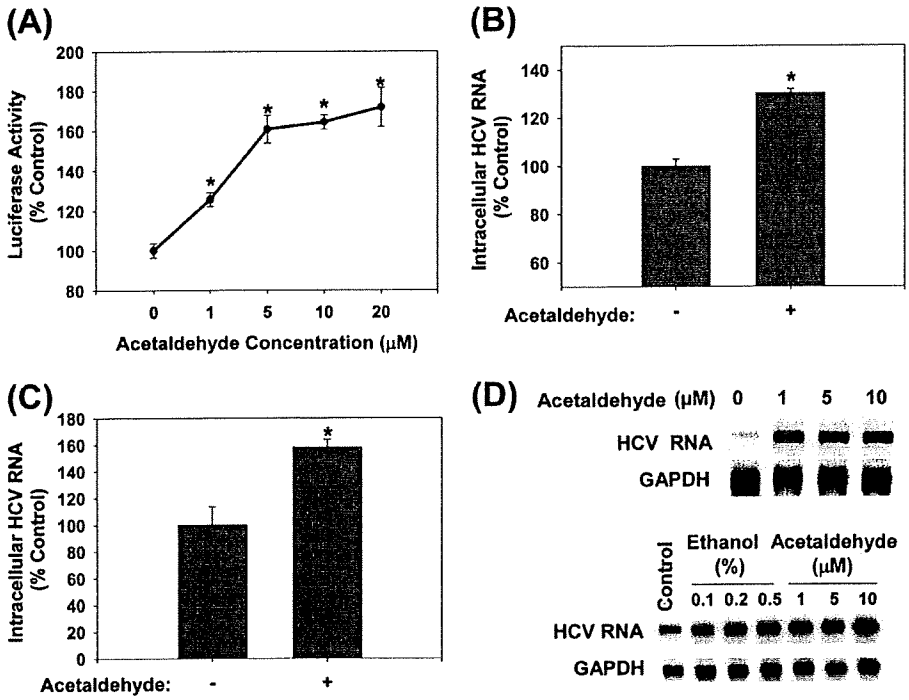

FIGURE 5. **Acetaldehyde increases intracellular HCV RNA.** SgJFH1-Luc (*A*) and JFH1 RNA-transfected cells (*B*), Huh7.5 cells inoculated with JFH1 virions (*C*), SgPC2 and Clone B cells (*D*) were incubated with acetaldehyde for 24 h and analyzed for HCV RNA by Northern blot or qRT-PCR ($n = 3$). *, indicates statistically significant difference for indicated sample size ($p < 0.05$).

inhibit mitochondrial β-oxidation and increase fatty acid synthesis (28). It is well-established that ethanol modulates fatty acid metabolism in part through NADH, and that this plays an important role in the development of steatosis in the alcoholic liver (28). Acetate and acetone would generate acetyl-CoA, which also drives lipogenesis (27, 28). Furthermore, cholesterol metabolism and fatty acid biosynthesis are important in HCV RNA replication (29). Lovastatin and fluvastatin, which are competitive inhibitors of 3-hydroxy-3-methyl-glutaryl-CoA reductase, and 5-(tetradecyloxy)-2-furoic acid (TOFA) and cerulenin, which inhibits fatty acid biosynthesis, have been shown to suppress the basal level of HCV replication (29, 30). Therefore, we next examined whether the potentiation of HCV RNA replication by above agents might be inhibited by modulators of lipid metabolism.

Lovastatin, fluvastatin, TOFA, and cerulenin almost completely inhibited the potentiation of HCV RNA replication by ethanol, acetaldehyde, isopropyl alcohol, acetone, and acetate (Fig. 7, *A* and *B*). In addition, inhibiting β-oxidation of fatty acids with β-mercaptopropionic acid caused a 15.2 ± 1.7-fold ($p < 0.01$) increase in HCV replication in these cells (Fig. 7*C*). Furthermore, ethanol, acetaldehyde, acetone, and acetate treatments increased the total intracellular cholesterol content, which was attenuated by lovastatin (Fig. 7*D*). Lactate, which increased NADH/NAD^+ without increasing HCV replication, had no significant effect on cholesterol levels (Fig. 7*D*). The data suggest that the elevation of HCV replication by ethanol, acetaldehyde, acetone, and acetate is mediated by increases in intracellular cholesterol and can be abrogated by the inhibition of cholesterol or fatty acid biosynthetic pathways.

DISCUSSION

High HCV titer is associated with the development and progression of liver diseases (31). In addition, ethanol consumption, high BMI, and high viral titer are strongly associated with poor response to anti-HCV therapy (32). Therefore, the increased HCV replication we saw with physiological levels of ethanol and acetaldehyde is likely to contribute to the pathogenesis and at least partly explain the negative effects that ethanol has on interferon-α therapy. Ethanol has been shown to suppress the antiviral function of interferon-α by interfering with the JAK-STAT signaling pathway (33); however, this is not likely to explain the potentiation of HCV replication we saw with ethanol because HCV effectively suppresses the type I interferon response in Huh7 cells. Additionally, ethanol and acetaldehyde could increase HCV replication in RIG-I-defective Huh7.5 cells (Fig. 5*C*, also, data not shown) (18, 34). Importantly, some ethanol treatments in this study were performed while wrapping cell culture dishes with parafilm to decrease loss of ethanol due to evaporation. However, we observed similar potentiation of HCV replication by ethanol, with and without the parafilm. The use of the parafilm also did not induce hypoxia as no significant change in the expression of hypoxia-inducible factor-1α could be found (data not shown).

Previously, it has been suggested that some of the key ethanol metabolizing enzymes might not be expressed in Huh7 cells (33). Indeed, we also found that alcohol dehydrogenase I is decreased in our Huh7 cells compared with human liver. However, CYP2E1 activity of our cells were within the normal range for human liver, and CYP2E1 expression could be enhanced by ethanol (Fig. 3). In addition, ethanol and acetaldehyde elevated the NADH/NAD^+ ratio, indicating that ethanol is being metabolized by our cells. Also, note that even though our cells do not have all of the normal ethanol metabolizing enzymes, our discovery that acetaldehyde and acetate can enhance HCV replication is significant as they bypass these reactions.

A previous study by Zhang *et al.* (3) using various chemical inhibitors of ethanol metabolism, suggested that some downstream metabolites of ethanol were involved in the potentiation of subgenomic HCV RNA replication by ethanol. Our data are in agreement with this study and suggest that ethanol and acetaldehyde also directly enhance HCV replication in the context of the complete viral replication cycle. In terms of the mechanism, we found that isopropyl alcohol, acetone, and acetate also increase HCV replication, and increased NADH/NAD^+ ratio was required for the potentiation of HCV replication by etha-

nol, acetaldehyde, as well as isopropyl alcohol, acetone, and acetate. In contrast, *t*-butanol, a tertiary alcohol that is poorly metabolized by humans and does not increase the NADH/NAD^+ ratio, did not elevate HCV replication, as predicted by our model (Fig. 6*B*). The NADH/NAD^+ ratio in ethanol-treated cells was decreased by cyanamide (Fig. 6*A*), suggesting that NADH is generated downstream of acetaldehyde (Fig. 3*A*). Acetate, the downstream metabolite of acetaldehyde, was previously considered inert but there is evidence that it can be converted to acetyl-CoA and other metabolic intermediates by mammalian cells (24, 28). Isopropyl alcohol is known to be metabolized into acetone and possibly other ketone bodies that can also be converted to acetyl-CoA (27). The mechanism by which isopropyl alcohol increases the NADH/NAD^+ ratio in our system is unclear and may involve residual ADH or hitherto uncharacterized enzyme activity that is induced by HCV.

In terms of how NADH increases HCV replication, NADH plays key roles in cellular bioenergetics and can modulate fatty acid synthesis as well as suppress β-oxidation (24, 28). We were interested in the potential involvement of lipids because HCV replicates in cholesterol-rich compartments in the cell, and cholesterol and fatty acid metabolism have been shown to be important for HCV replication (29). Specifically, cholesterol metabolism increases basal HCV replication by the geranylgeranylation of FBL2 (29). We found that inhibiting the host mevalonate pathway with statins and fatty acid synthesis with TOFA or cerulenin blunted the potentiation of HCV replication by ethanol, acetaldehyde, isopropyl alcohol, acetone, and acetate, whereas inhibiting β-oxidation dramatically increased HCV replication (Fig. 7). In addition, the potentiation of HCV replication by these agents was accompanied by an increase in the intracellular cholesterol content, which was attenuated by lova-

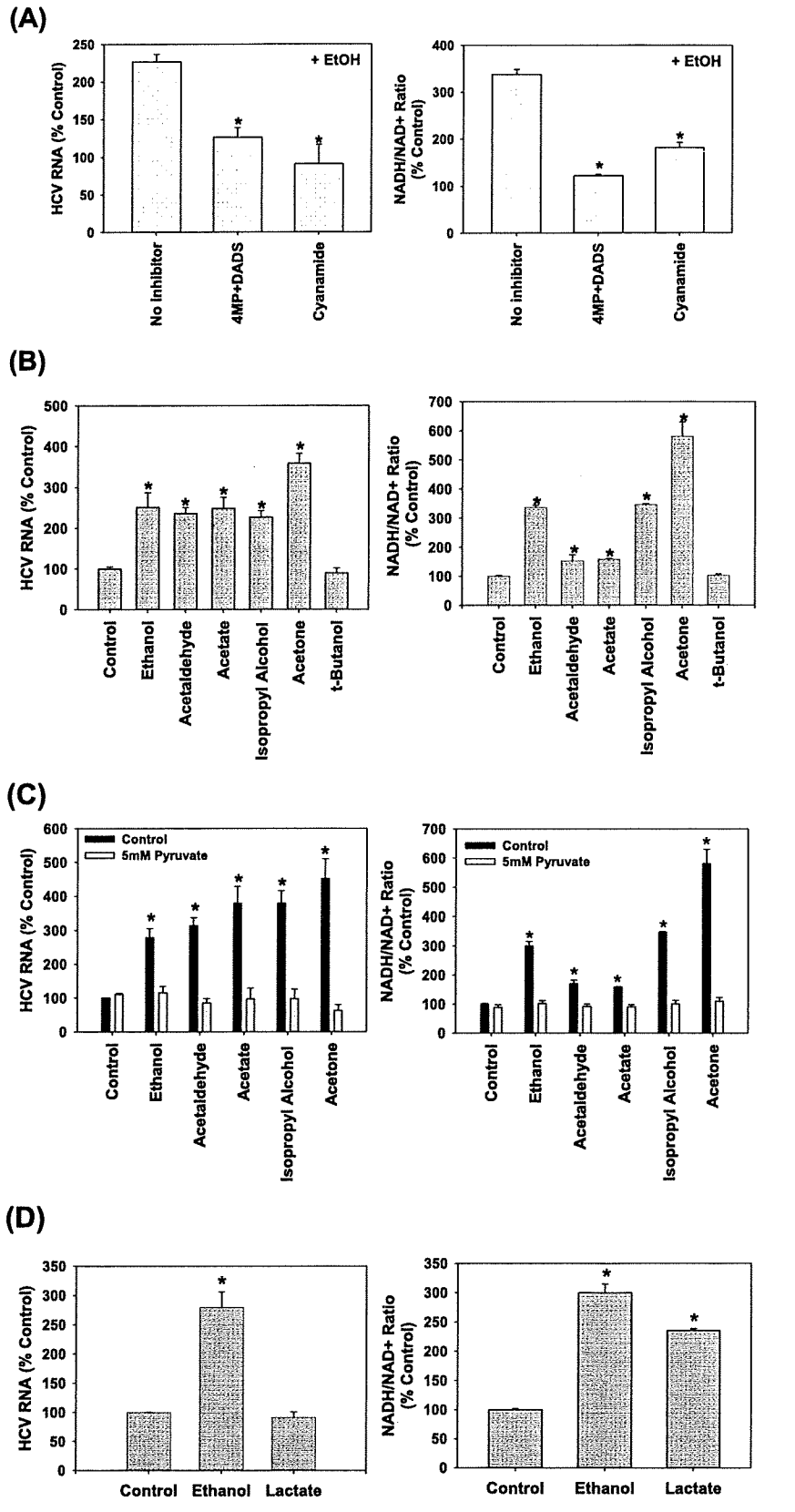

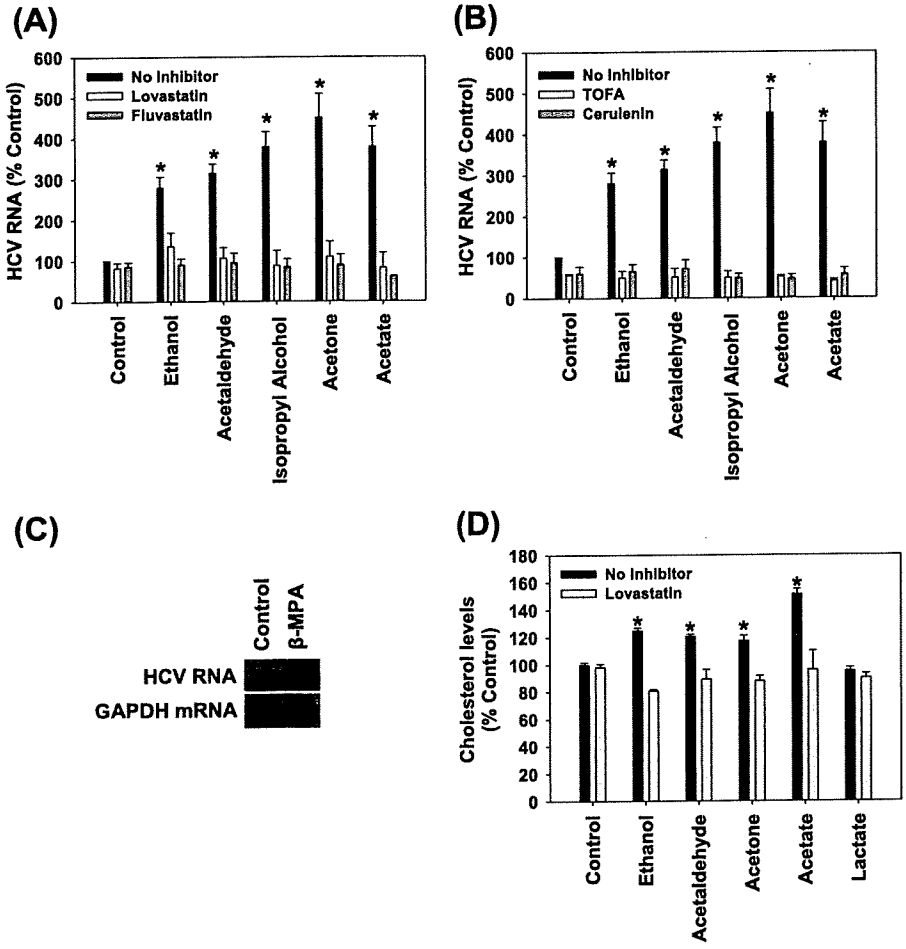

FIGURE 7. **Role of lipogenesis in the enhancement of HCV replication by ethanol, acetaldehyde, isopropyl alcohol, acetone, and acetate.** SgPC2 cells were treated for 24 h with (*A* and *B*) 0.2% ethanol, 5 μM acetaldehyde, 0.2% isopropyl alcohol, 2 mM acetone, 5 μM acetate ± 30 min pretreatment with (*A*) 5 μM lovastatin, 5 μM fluvastatin, (*B*) 5 μg/ml TOFA, 5 μg/ml cerulenin, or with (*C*) 2 mM β-mercaptopropionic acid (β-MPA). Then, HCV RNA levels were monitored by Northern blot and quantified by densitometry (n = 3). *D*, SgPC2 cells, treated for 24 h with ethanol, acetaldehyde, acetone, and acetate ± lovastatin, were monitored for cholesterol levels (n = 3). Lovastatin was activated, as described, before use (29). *, indicates statistically significant difference for indicated sample sizes ($p < 0.05$).

statin (Fig. 7*D*). Regarding potential effects of NADH on the ATP, overall ATP levels were not significantly perturbed in these cells by ethanol or other treatments (data not shown), suggesting that ATP is not likely to explain the effects that ethanol had on HCV. In fact, ethanol also increased the rate of HCV replication in the *in vitro* replication assay (Fig. 2*C* and 2*D*) which was performed in the presence of excess ATP. Taken together, these data indicate that the potentiation of HCV replication by ethanol, acetaldehyde, acetate, isopropyl alcohol, and acetone ultimately requires host lipid metabolism and is sensitive to lipid modulators, which points to potential targets for therapy. The concentrations of lovastatin and fluvastatin used here are higher than the doses used clinically to treat hypercholesterolemia. However, it is possible that statins, if used in combination with antivirals or other lipid modulators, will help control HCV replication, particularly in chronic alcoholics who show resistance to standard anti-HCV therapy (35). It is also interesting to note that the concentrations of acetone that enhanced HCV replication in this study are physiological levels that can be attained during metabolic dysfunction such as diabetes and during starvation (27), and HCV infection can lead to insulin resistance (36). In addition, acetate, which increased HCV replication at μM to mM concentrations in this study (Fig. 6*B* and data not shown), is used in hemodialysis.

Interestingly, increasing the NADH/NAD$^+$ ratio with lactate was not sufficient to increase HCV replication, suggesting that other factors may also play a role (Fig. 7*D*). Lactate also did not increase the intracellular cholesterol level. These results are consistent with an important role of cholesterol in the regulation of HCV replication. The data also indicate that even though ethanol and lactate both increase the NADH/NAD$^+$ ratio, ethanol is more lipogenic than lactate in these cells. The reason for these differences is unclear but it might be explained at least in part by the fact that ethanol can inhibit citric acid cycle as well as gluconeogenesis, which may cause acetate/acetyl-CoA produced by ethanol metabolism to be shunted more toward the lipogenic pathways, whereas these processes are likely to be stimulated by lactate (37). Ethanol can also decrease the total oxidation of fatty acids to CO_2, and increase the breakdown of glycogen, which may further drive lipogenesis in these cells (37–39). Further investigation into these effects will be beneficial to understanding how different metabolic conditions would affect HCV replication in hepatocytes.

Recently, McCartney *et al.* (7) reported an elevation of HCV RNA by ethanol in Huh7 replicon cells, transfected with

FIGURE 6. **Role of NADH/NAD$^+$ in the potentiation of HCV replication by ethanol, acetaldehyde, acetate, isopropyl alcohol, and acetone.** SgPC2 cells, supporting Con1 subgenomic HCV RNA replication, were treated with (*A*) 0.2% ethanol ± 0.1 mM 4MP plus 25 μM DADS or 0.1 mM cyanamide (n = 3); (*B*) 0.2% ethanol, 5 μM acetaldehyde, 5 μM acetate, 0.2% isopropyl alcohol, 2 mM acetone, or 25 mM *tert*-butanol (n = 4); (*C*) 0.2% ethanol, 5 μM acetaldehyde, 5 μM acetate, 0.2% isopropyl alcohol, and 2 mM acetone, with and without 5 mM pyruvate (n = 3); or (*D*) 0.2% ethanol or 5 mM lactate for 3 h for NADH/NAD$^+$ ratio measurement or 24 h for HCV RNA levels. HCV RNA levels were monitored by Northern blot (*A–D, left panels*). NADH/NAD$^+$ ratios were measured by an enzymatic NADH recycling assay, as described under "Experimental Procedures" (*A–D, right panels*). Northern blots were quantified by densitometry. *, indicates statistically significant difference for indicated sample sizes ($p < 0.05$).